IEEE Access
Multidisciplinary | Rapid Review | Open Access Journal

Received 22 November 2024, accepted 14 January 2025, date of publication 20 January 2025, date of current version 27 January 2025.

*Digital Object Identifier 10.1109/ACCESS.2025.3532393*

RESEARCH ARTICLE

# A Novel Air-to-Ground Communication Scheme for Advanced Big Data Collection in Smart Farming Using UAVs

**GEORGIOS A. KAKAMOUKAS[1], THOMAS D. LAGKAS[2], VASILEIOS ARGYRIOU[3], SOTIRIOS K. GOUDOS[4], (Senior Member, IEEE), PANAGIOTIS RADOGLOU-GRAMMATIKIS[1], (Member, IEEE), STAMATIA BIBI[1], AND PANAGIOTIS G. SARIGIANNIDIS[1], (Member, IEEE)**

[1]Department of Electrical and Computer Engineering, University of Western Macedonia, 501 50 Kozani, Greece
[2]Department of Informatics, Democritus University of Thrace, Kavala, Greece
[3]Department of Networks and Digital Media, Kingston University, KT1 1LQ London, U.K.
[4]ELEDIA@AUTH, School of Physics, Aristotle University of Thessaloniki, 541 24 Thessaloniki, Greece

Corresponding author: Sotirios K. Goudos (sgoudo@physics.auth.gr)

This work was supported by European Union's Horizon Europe Research and Innovation Programme [Autonomous and Self-organized Artificial Intelligent Orchestrator for a Greener Industry 4.0 (TALON)] under Grant 101070181.

**ABSTRACT** The evolution of Flying Ad Hoc Networks (FANETs) demands the development of advanced routing protocols that can address the unique challenges associated with Unmanned Aerial Vehicle (UAV) missions. This paper proposes a novel Air-to-ground, Energy-awaRe, mission-Oriented protocol, leveraging Fuzzy Logic (AERO-FL), to enhance UAV cooperation and optimize network performance in deterministic scanning operations. The study focuses on a Smart Farming (SF) scenario for extensive crop surveillance, which traditionally relies on a single UAV. This conventional approach is often inefficient because of its inability to enable real-time data transmission and its vulnerability to operational failures. The proposed system replaces the single UAV approach with a cooperative FANET comprising multiple UAVs, significantly reducing mission completion time while facilitating real-time data transmission through the cooperation of aerial and ground nodes. The simulation results demonstrate that AERO-FL outperforms established routing protocols in key performance metrics. These findings underscore the potential of AERO-FL in a variety of scanning applications, including traffic monitoring, environmental observation, disaster response, and military operations. By enabling UAV cooperation in a mission-oriented routing framework, this study provides a foundation for future research aimed at achieving full FANET capabilities.

**INDEX TERMS** Flying ad hoc networks, air-to-ground communication, routing protocols, fuzzy logic, smart agriculture, network simulations, ns3.

## I. INTRODUCTION

An Unmanned Aerial Vehicle (UAV), commonly referred to as a drone, is an autonomous aircraft capable of operating without an onboard human pilot [1]. This autonomy enables UAVs to perform cost-effective missions while mitigating risks to human lives. UAVs can be operated remotely through commands from a Ground Control Station (GCS) or perform autonomous tasks using onboard systems, including autopilots and sensors such as the Global Positioning System (GPS) and Inertial Measurement Units (IMU) [2].

UAVs have gained attention in the military and civilian domains due to their stability, endurance, and adaptability in various operations [3]. Integrating UAVs with emerging technologies, including the Internet of Things (IoT), 5G, and Beyond 5G networks, has further expanded their application spectrum [4]. During the past decade, UAVs have been widely deployed in areas such as object detection, public safety, traffic monitoring, military operations, hazardous environment exploration, navigation, atmospheric data collection, disaster

The associate editor coordinating the review of this manuscript and approving it for publication was Xijun Wang.

recovery, healthcare, data transmission, infrastructure monitoring, emergency management, cargo transport, wildfire surveillance, and logistics [5].

Flying Ad hoc Networks (FANETs) are a specialized subset of Mobile Ad hoc Networks (MANETs) designed to enable communication among UAVs [6], [7]. FANETs are particularly promising for applications that require UAV coordination and collaboration, offering advantages in cost effectiveness and operational safety [8]. These networks have been proposed for various domains, including agriculture [9], transportation [10], military operations [11], healthcare [12], and surveillance [13]. However, routing within FANETs remains a significant challenge due to the highly dynamic topology, frequent link disruptions, variable node density, resource constraints, and the impact of 3-Dimensional (3D) mobility patterns [14]. Routing involves identifying optimal paths for data transmission between source and destination nodes. This task becomes increasingly complex in FANETs due to their dynamic topology, three-dimensional operational environment, and rapid node mobility [15].

Previous studies have explored FANET routing using simulation-based evaluations [16]. These studies have highlighted critical challenges, such as frequent topology changes, limited connection stability, and energy constraints due to mobility, size, weight, and energy consumption of UAVs [17]. However, many of these studies rely on simplistic stochastic mobility models, such as pure randomized and time-dependent models, which fail to capture the structured and goal-oriented nature of UAV missions [18]. By definition, stochastic models depend on random processes to simulate node movement, making them less suitable for real-world applications such as military operations, traffic monitoring, or agricultural surveying, where UAVs follow predetermined routes [16]. The representativeness of a mobility model, its ability to accurately simulate mission-specific UAV behaviors, is crucial for realistic network performance evaluations. Stochastic models can fail in this regard, leading to simulation results that may not align with real-world scenarios. In contrast, the use of mobility models tailored to specific applications can provide more accurate and reliable insights into network performance [19]. This highlights the need for deterministic mobility models that will be able to capture the movement behavior of a UAV, in order to evaluate FANET performance effectively.

This paper introduces AERO-FL, a mission-oriented reactive routing protocol that incorporates Artificial Intelligence (AI) features through fuzzy logic. Depending on the foundational principles of Ad hoc On-Demand Distance Vector (AODV) routing protocol [20], AERO-FL introduces advanced decision-making capabilities that take into account factors such as intrinsic node attributes, UAV connectivity, and network topology. This optimization improves data forwarding and resource management within the network. To evaluate its performance, AERO-FL is tested using a three-dimensional mobility model, newly proposed in this study and accurately reflects UAV movement in scanning scenarios. Simulations performed using the Network Simulator-3 (NS-3) indicate that AERO-FL achieves superior performance compared to existing routing protocols for scanning operations.

## II. RELATED WORK

In recent years, there has been a surge in efforts aimed at developing new routing protocols integrated with new features, such as fuzzy logic. Most of these efforts have been focused on the MANET environment. Among existing routing protocols, AODV stands out as a robust and widely recognized solution that has garnered significant attention in the realm of ad hoc networks. Consequently, many of the newly proposed routing protocols have been built on the foundational principles of AODV, leveraging its established framework and capabilities as a solid starting point for further innovation and enhancement.

The authors in [21] propose a novel approach based on fuzzy logic to improve the route selection scheme in MANETs, acknowledging the intricate interplay of multiple route selection criteria influencing network performance. Leveraging fuzzy logic is an effective strategy to build optimal routes, mitigating the limitations of single-metric routing protocols. Comparative evaluations against traditional AODV routing protocols reveal superior performance metrics achieved by the proposed fuzzy logic-based AODV routing protocol, particularly in dynamic and high-mobility environments. The simulation results demonstrate significant improvements in throughput and packet delivery, along with a reduced end-to-end delay compared to its predecessors.

Taking into account factors such as delay, stability and remaining energy of nodes, the authors in [22] introduce a novel fuzzy logic-assisted variant of the AODV routing algorithm, denoted as FL-AODV, aimed at enhancing route reliability in MANETs. In the route discovery phase, the algorithm selects the node with the highest reliability as the relay node, thereby reserving the route with the highest accumulated reliability for data transmission. The simulation results indicate that the proposed routing protocol exhibits superior reliability compared to the traditional AODV protocol and the Fuzzy Logic Routing Algorithm (FLRA) while maintaining a low delay. Specifically, the proposed protocol demonstrates enhanced link connectivity and prolonged route lifespan, with an average routing reliability approximately 18% higher than that of traditional AODV.

The authors in [23] introduce the Fuzzy Control Energy Efficient (FCEE) routing protocol as a solution to address the challenges encountered in wireless mesh networks. By integrating the AODV protocol with fuzzy logic techniques, FCEE aims to improve both network lifetime and performance. The proposed approach incorporates a memory-based channel integrated with fuzzy logic methodologies, which effectively regulates the forwarding of broadcast packets based on the energy availability of the operating node.

To assess the effectiveness of the FCEE protocol, the article compares its performance with two routing protocols: AODV and Intelligent Routing AODV (IRAODV). The simulation results show that the FCEE routing protocol significantly enhances the reliability of the conventional AODV, offering improved link connectivity and prolonged route lifetimes.

Moreover, the authors in [24] introduce a fuzzy logic-based ad hoc on-demand distance vector (FL-AODV) routing protocol, which employs a multivariate cross-layer design architecture to optimize multiple performance parameters in wireless ad hoc networks. The proposed fuzzy optimization framework utilizes inputs from four different layers of the Open Systems Interconnection (OSI) model, including the header length from the data link and physical layers, route timeout from the network layer, and node mobility speed from the application layer. Additionally, parameters such as the bit rate for the application layer and the communication range for the data link layer are considered as the fuzzy outputs derived from the defuzzifier. The routing protocol is evaluated through simulation experiments under diverse node mobility conditions. Various network performance metrics, including reception cache hit, packet delivery ratio, packet errors, ping loss rate, mean throughput, and delay, are computed and analyzed to compare FL-AODV with traditional AODV routing mechanisms. The performance of the proposed fuzzy routing model showcases its efficacy in terms of throughput and delay.

An intelligent routing protocol tailored specifically for Vehicles Ad hoc Networks (VANETs), with a focus on selecting stable routes using fuzzy logic, is proposed in [25]. The approach endows each network node with autonomous decision-making capabilities, enabling route selection based on crucial factors such as vehicle mobility rates and available bandwidth. A comparative study was deployed against AODV protocol. The simulations indicate superior performance of the proposed protocol. The results underscore the potential of the approach to enhance routing efficiency and network performance in dynamic vehicular environments.

The authors in [26] introduce the Adaptive Fuzzy Logic Inspired Path Longevity Factor-Based Forecasting Model (AFLIPLFFM) as a predictive tool aimed at enhancing path stability, thereby improving network throughput and packet delivery ratio. The AFLIPLFFM model operates by initially computing the Instantaneous Path Reliability (IPR) of mobile nodes. Subsequently, this IPR value is fed into a fuzzy inference engine, which employs a set of ''if-then'' rules defined based on triangular membership functions to calculate the path stability output. Through extensive experimentation, the efficacy of the AFLIPLFFM protocol is demonstrated in reducing end-to-end delay under varying node densities. Specifically, the proposed protocol showcases a noteworthy reduction in end-to-end delay, with reductions of 5.69%, 7.16%, and 9.18% observed compared to the Energy and active new Neighbor rate-based Routing Protocol (EN2RP), Ad hoc On demand Multipath Distance Vector (AOMDV), and AODV protocols, respectively. Their results underscore the potential of AFLIPLFFM in optimizing network performance and minimizing delays, thereby contributing to enhanced reliability and efficiency in ad hoc network operations.

To address the broadcast problem encountered in ad hoc networks, authors in [27] introduce the Cross-layer Adaptive Fuzzy-based Ad hoc On-Demand Distance Vector (CLAF-AODV) routing protocol. CLAF-AODV integrates a two-level fuzzy logic framework to suppress broadcast packets within the network. The CLAF-AODV protocol takes into account various factors, including stability, quality, and adaptability, to decide on the forwarding of broadcast packets. To achieve this, the protocol dynamically calculates the forwarding probability considering parameters such as node quality, path quality, and network density surrounding each node. Utilizing fuzzy logic, the protocol evaluates node quality based on multiple inputs including energy level, available bandwidth, queue length, signal strength, and MAC contention. Through simulation and analysis, the findings reveal that the CLAF-AODV routing protocol outperforms both the original AODV and Fixed Probability AODV (FP-AODV) protocols. The proposed protocol demonstrates significant reductions in routing load and MAC layer contention, particularly in scenarios characterized by high network density. Moreover, CLAF-AODV exhibits superior performance metrics including throughput, packet loss, and end-to-end delay compared to the other routing protocols evaluated in this study.

Recent efforts have been undertaken to devise and implement novel routing protocols tailored also for FANETs [28].

The authors in [29] introduce a fuzzy logic-based routing scheme tailored for FANETs, which encompasses two distinct phases: route discovery and route maintenance. In the initial phase, they propose a technique for computing the score of each node within the network, aimed at mitigating the broadcast storm problem and curtailing the proliferation of control messages typically associated with the route discovery process. This scoring mechanism relies on various parameters including movement direction, residual energy levels of the nodes, the quality of the link and the stability of the nodes. Furthermore, during the route selection process, they devise a fuzzy system to prioritize routes based on their ''fitness'', minimizing delay, hops, and other relevant factors crucial for efficient data transfer. The second phase comprises two critical steps: proactive measures to forestall route failures by promptly identifying and adjusting paths nearing the failure threshold, and reactive procedures for swiftly reconstructing failed routes, ensuring seamless network connectivity. The simulation results are juxtaposed with those obtained from three existing routing protocols, namely Energy-efficient Connectivity-aware Data Delivery (ECaD), Link stability estimation-based preemptive routing (LEPR), and AODV. The comparative analysis shows that the

proposed routing method outperforms the existing schemes in various performance metrics including end-to-end delay, packet delivery rate, route stability, and energy consumption. However, it is important to note that there is a slight increase in routing overhead associated with the proposed approach.

The authors in [30] introduce a multi-objective routing algorithm tailored also for FANETs. Recognizing the unique dynamics of FANETs, authors propose the integration of Q-learning-based fuzzy logic into the routing protocol. The proposed algorithm streamlines the selection of routing paths by evaluating both link and overall path performances. Each UAV autonomously determines the optimal routing path to the destination using a fuzzy system equipped with link-level and path-level parameters. The link-level parameters encompass critical factors such as transmission rate, energy state, and inter-UAV connectivity status, while the path-level parameters encompass metrics like hop count and successful packet delivery time. Furthermore, the path-level parameters undergo dynamic updates through a reinforcement learning mechanism. The simulation results validate the effectiveness of the proposed approach by comparing it with conventional fuzzy logic and Q-value-based ad hoc on-demand distance vector protocols. The findings demonstrate that the proposed method consistently maintains low hop counts and energy consumption levels, thereby extending the network's operational lifetime.

A drone-assisted Distributed routing protocol in IoT environments (D-IoT) is introduced in [31]. This protocol is specifically tailored to enhance network performance in IoT environments by prioritizing Quality of Service (QoS) provision. To optimize QoS provision in UAV-centric networks, the authors derived parameters such as the relative velocity of drones, expected link availability period, residual route load capacity, and route delay. Leveraging a neuro-fuzzy inference system, they integrate these parameters to facilitate reliable and efficient route selection. Subsequently, they develop a UAV-assisted distributed routing framework based on the established UAV mobility model and QoS parameters. Simulation results demonstrate the superior performance of D-IoT compared to existing protocols, indicating its potential applicability in various domains such as agriculture, traffic management, and border monitoring with drones.

Table (1) summarizes recent efforts of researchers to improve popular ad hoc routing protocols by incorporating fuzzy logic from 2020 and onward. The table details the environments and types of movement for which these protocols were tested, the fuzzy inputs used, and the results achieved.

A notable observation is that all of these protocols have only been tested using stochastic mobility models. As highlighted in [13] and [18], stochastic mobility models are considered less suitable for practical FANET applications and more appropriate for scientific and exploratory purposes. This lack of attention to deterministic mobility models, which have been shown to be better at simulating UAV movements in real FANET applications, as shown in studies like [13], is evident. Moreover, scanning movement represents one of the most prevalent motion patterns in real-world UAV scenarios, as it supports a wide array of practical applications, including search and rescue missions, military reconnaissance, environmental monitoring, agricultural management, traffic surveillance, and others [19].

The research question that this article addresses is articulated as follows:

How can the integration of fuzzy logic enhance the performance of routing protocols in FANETs, particularly during scanning operations in a 3D simulation environment that incorporates realistic UAV mobility and collaboration between aerial and ground nodes?

This paper answers the research question by developing a comprehensive simulation environment tailored to evaluate routing protocols in FANETs under realistic UAV mobility scenarios, specifically focusing on scanning operations. Unlike traditional approaches that rely on stochastic mobility models, this work employs a novel deterministic 3D mobility model that accurately represents UAV behaviors and mission-specific dynamics. The simulation framework incorporates collaborative interactions between aerial and ground nodes, taking advantage of their distinct attributes, such as altitude, mobility, and connectivity, to effectively mirror real-world scenarios. In addition, the paper introduces a newly designed routing protocol that integrates fuzzy logic to enhance decision-making capabilities. This protocol considers critical factors, including the type of node (aerial or ground), mobility status (static or mobile), connectivity, and network topology. By evaluating the proposed protocol against well-established ad hoc routing protocols in the context of scanning operations, the paper demonstrates the advantages of fuzzy logic in facilitating more reliable, efficient and context-aware routing in FANETs. Through these contributions, the research not only addresses the identified gaps but also provides insights for advancing FANET communication strategies in dynamic and complex operational environments.

An additional advantage of the current is the fact that unlike previous studies that used the outdated ns-2 simulator with limited three-dimensional capabilities [18], this research uses the more advanced ns-3 simulator. Using ns-3 ensures more reliable and accurate simulation results, offering greater power and flexibility, as noted in recent publications [32].

## III. ROUTING PROTOCOLS

Routing protocols play a pivotal role in the establishment and maintenance of communication paths in networks where nodes dynamically form temporary networks without the use of fixed infrastructure (called ad hoc networks) [33]. These protocols facilitate the efficient transmission of data packets between the source and destination nodes, overcoming the challenges posed by the dynamic and often unpredictable nature of these networks [34]. Several routing protocols have been developed to address the unique challenges of ad hoc networks. Among the most popular are the AODV [20], Destination-Sequenced Distance Vector

**TABLE 1. Comparative analysis of fuzzy Logic-Enhanced AODV variants in Ad Hoc networks (2020 - 2023).**

| Reference | Network | Movement | Fuzzy Inputs | Work Features |
|---|---|---|---|---|
| [21] | MANET | Stochastic | Residual Energy, Speed, Hop-Count, Bandwidth, Expiration Time | Enhanced Packet Delivery Ratio and Throughput / Decreased End-to-End Delay |
| [22] | MANET | Stochastic | Stability | Enhanced Packet Delivery Ratio / Decreased Routing Overhead and End-to-End Delay |
| [23] | Wireless Mesh Networks | Stochastic | Residual Energy | Prolonged Route Lifetime |
| [24] | MANET | Stochastic | Header Length, Route Timeout, Node Speed | Enhanced Throughput / Decreased End-to-End Delay |
| [29] | FANET | Stochastic | Node Movement, Residual Energy | Decreased End-to-End Delay, and Energy Consumption, Enhanced Packet Delivery Ratio / Increased Overhead |
| [25] | VANET | Stochastic | Vehicle Mobility, and Bandwidth | Enhanced Packet Delivery Ratio / Decreased End-to-End Delay |
| [26] | MANET | Stochastic | Instantaneous Path Reliability | Decreased End-to-End Delay |
| [27] | MANET | Stochastic | Residual Energy, Signal Strength, Bandwidth, Network Density | Decreased Routing Overhead, and End-to-End Delay, Enhanced Throughput |
| [30] | FANET | Stochastic | Transmission Rate, Residual Energy, Hop-Count, Successful Packet Deliveries | Prolonged Route Lifetime |
| [31] | FANET | Stochastic | Node Movement, Link Availability Period, Residual Load Capacity, Delay | Enhanced Throughput / Decreased End-to-End Delay |

(DSDV) [35], and Optimized Link State Routing (OLSR) [36] protocols.

AODV is a reactive routing protocol that establishes routes between nodes only when needed. When a node requires a route to a destination, it initiates a route discovery process by broadcasting Route Request (RREQ) packets. Intermediate nodes forward these packets until they reach the destination or a node with a fresh route to the destination. Upon receiving the RREQ, nodes create route entries in their routing tables and reply with Route Reply (RREP) packets. AODV utilizes sequence numbers to ensure the freshness of routing information and prevent routing loops. DSDV is a proactive routing protocol based on the classical Bellman-Ford algorithm. In DSDV, each node maintains a routing table containing entries for all reachable destinations in the network. These entries include the next-hop node and an associated sequence number, which is periodically updated to reflect changes in the network topology. DSDV employs sequence numbers to ensure that nodes have the most recent routing information and to prevent routing loops. To maintain routing table consistency, nodes periodically broadcast their routing tables to their neighbors, and upon receiving an update, nodes compare the sequence numbers of routes to update their routing tables accordingly. OLSR is also a proactive routing protocol that maintains an up-to-date view of the network topology by periodically exchanging link-state information with neighboring nodes. Each node selects a set of Multi-Point Relay (MPR) nodes responsible for forwarding control messages, reducing overhead. OLSR utilizes two types of control messages: Hello messages for neighbor detection and MPR selection, and Topology Control (TC) messages for disseminating topology information. OLSR is particularly suitable for large-scale networks with high node density.

These routing protocols have been extensively studied and implemented in various ad hoc network scenarios, each offering unique advantages and trade-offs in terms of performance, scalability, and adaptability to network conditions [37]. Numerous variations of the aforementioned routing protocols have emerged to address various scenarios, encompassing varying movement patterns and accommodating hybrid communication paradigms such as air-to-ground communication [38]. These adaptations have introduced a spectrum of mechanisms tailored to handle the aforementioned scenarios. These mechanisms range from simple adjustments in route discovery intervals to sophisticated implementations integrating AI into the decision-making process for selecting the next hop [39].

## IV. FUZZY LOGIC BASICS

Research and empirical investigations have shown that achieving precise measurement, modeling, and control of real-world applications can be challenging due to factors such as incomplete and stochastic data samples [40]. Fuzzy logic emerges as a mathematical tool aimed at addressing these complexities by striving to mimic human cognitive processes. Fuzzy logic theory offers a paradigm shift from classical set theory by introducing the notion of fuzzy sets. Unlike classical sets, which operate within a framework of precise and unequivocal membership functions, fuzzy sets introduce the concept of partial membership. This paradigm shift allows elements to exhibit varying degrees of belongingness to a set, enabling a more nuanced representation of uncertainty. Consequently, outcomes in fuzzy logic are not confined to binary true or false values but rather embrace the spectrum of partial truth or falsity.

Consider a reference set denoted by $X$ that comprises a multitude of members denoted by $x$. Equation (1) delimits the establishment of fuzzy set $A$, derived from reference set $X$, in the following manner.

$$A = \{(x, \mu_A(x)) \,|\, x \in X\} = \sum_{i=1}^{n} \mu_A(x_i)/x_i \qquad (1)$$

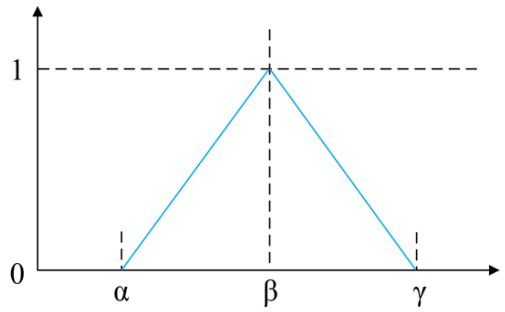


**FIGURE 1.** The triangular membership function.

where, $\mu_A(X) \rightarrow [0,1]$ is membership function of $A$ and $\mu_A(x_i)$ represents the membership degree of the element $x_i$ in $A$. Note that the symbol "/" does not refer to a division operation. It is just a symbol for separating the membership degree and the corresponding member. Within a fuzzy set, the membership functions assume pivotal roles. Among the key functions are triangular, trapezoidal, and Gaussian. In this research work, the focus shifts to a single primary membership function, triangular, as it aligns with the framework of the proposed routing protocol.

The triangular membership function is known by three parameters, including $\alpha$, $\beta$, and $\gamma$, so that $\alpha < \beta < \gamma$ as shown in Fig. (1).

The triangular membership function is defined based on Equation (2):

$$\mu(x) = MAX\left(min\left(\frac{x-\alpha}{\beta-\alpha}, \frac{\gamma-x}{\gamma-\beta}\right), 0\right) \tag{2}$$

As shown in Fig. (2) within a fuzzy system, pivotal modules include the fuzzifier related to input fuzzyfication, defuzzifier related to output defuzzyfication, rule base, and fuzzy inference engine. The fuzzifier plays a crucial role in converting system inputs into fuzzy inputs, determining a membership degree for each fuzzy input. The fuzzy inference engine computes fuzzy values, operating directly with the rule base which contains a collection of "if-then" rules. The results of the inference engine are fuzzy variables. Lastly, the defuzzifier, transforms fuzzy outputs into crisp values, employing various approaches such as averaging or centroid schemes.

## V. MISSION SCENARIO AND NETWORK MODEL

Modern crop surveying and mapping often utilize UAVs, satellites, and ground-based sensors [41]. UAVs, equipped with high-resolution cameras and sensors, are particularly effective in capturing georeferenced images and data over large areas [19]. The information collected is then processed using Geographic Information Systems (GIS) and other software tools to create comprehensive maps and reports [42]. Fig. (3) illustrates several potential export types generated by GIS. Fig. (3a) displays a five-band composite, including green, red, red-edge, near-infrared (NIR), and alpha bands. This multi-spectral image provides valuable information about the vegetation and land cover. Fig. (3b) represents the Digital Surface Model (DSM), depicting variations in terrain height and surface features. Fig (3c) shows the orthomosaic, which is a geometrically corrected high-resolution aerial photograph stitched together from multiple images. Fig. (3d) presents the Normalized Difference Vegetation Index (NDVI) map, a widely used metric to assess crop health by measuring vegetation density and vigor. Each of these results has been meticulously constructed from individual images to generate the comprehensive outputs displayed. The GIS software can produce different types of exports tailored to the specific informational needs of stakeholders, thereby providing versatile and actionable insights for various applications.

Current methods for crop surveying and mapping with UAVs typically involve a single UAV scanning a predefined area and collecting image data. This traditional approach can be divided into three main stages:

1) Flight Preparation Stage:
   - Flight Analysis and Planning: This preliminary step involves analyzing the mission specifications and preparing the UAV accordingly. Inputs include the coordinates of the surveyed area, the mobility model, the flight altitude, and the necessary equipment.
2) Flight Operation Stage:
   - Flight Initiation – Takeoff: The UAV is transported to the mission's starting point and takes off.
   - Data Acquisition: Upon reaching the desired altitude, the UAV begins collecting images of the crop.
   - Data Storage: Each image is stored on an SD card within the UAV.
   - Battery Level Check: The UAV's battery level is periodically monitored. If the battery drops below a predefined threshold or there is a rapid decline, the UAV must land for a battery replacement.
   - SD Card Memory Check: The available memory on the SD card is also checked periodically. If the memory is full, the UAV must land to replace the SD card with an empty one.
   - Flight Termination – Landing: Once the UAV completes its mission, it lands at a predefined point.
3) Post-Flight Data Exploration Stage:
   - Data Extraction: The SD card(s) are removed from the UAV and inserted into a ground workstation, where the image data, often amounting to gigabytes, are extracted and stored.
   - Data Exploitation: The image data are processed using software that merges the images based on geolocation information to create a single mosaic image illustrating the entire surveyed area.
   - Results: The mosaic along with other types of images, are analyzed and used by stakeholders for reference and decision-making.

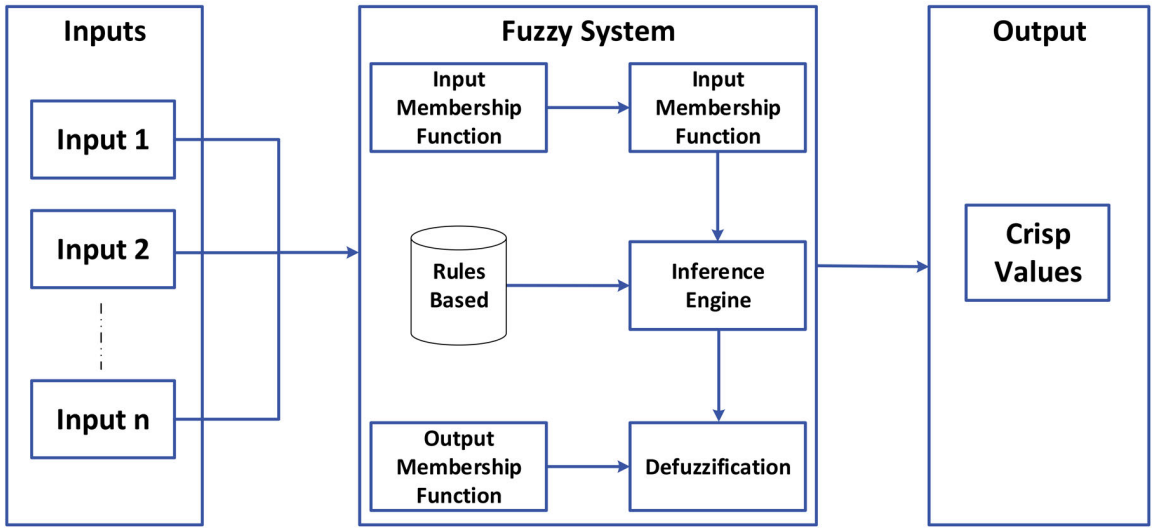


**FIGURE 2.** Fuzzy system structure.

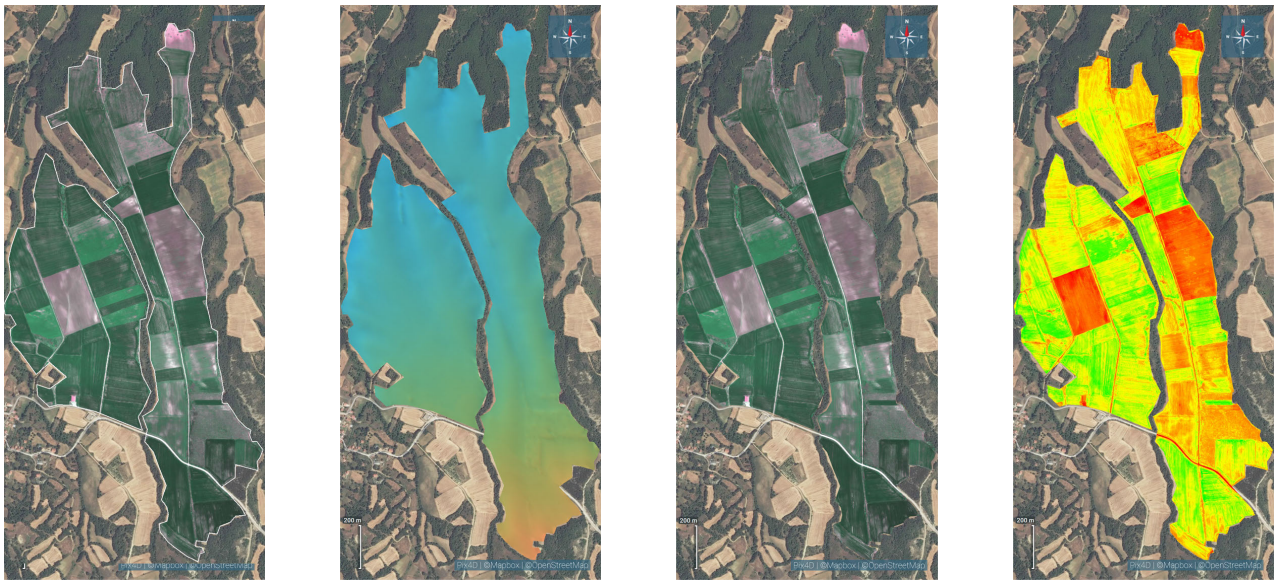

(a) (b) (c) (d)

**FIGURE 3.** Four different types of images generated by a Geographic Information System (GIS) software a) Five-band composite b) Digital Surface Mode (DSM). c) Orthomosaic and d) Normalized Difference Vegetation Index (NDVI).

This traditional approach raises the following concerns:

1) The cost of a single UAV capable of carrying the necessary hardware and scanning the entire field with minimal battery and SD card changes is tens of thousands of euros.
2) The mission execution time is limited by the UAV's capabilities, and extended by the need for battery and SD card replacements.
3) The risk of a single point of failure in the UAV can result in mission cancellation.
4) The mission requires significant manual intervention, such as changing batteries and SD cards and extracting image data to the ground workstation.

The proposed scenario addresses these concerns by employing an ad hoc network comprising a FANET and ground static nodes arranged in a grid. Multiple mini UAVs within the FANET acquire and forward image data through the FANET and ground network to a ground workstation, which performs all necessary analyses to provide stakeholders with final information. This approach divides the crop surveying process into the following stages:

1) Flight Preparation Stage:
   - Flight Analysis and Planning: This step involves analyzing the mission specifications and preparing each UAV accordingly. Inputs include the coordinates of the surveyed area, the mobility model, the flight altitude, and the necessary equipment for each UAV.

2) Flight Operation Stage:
   - Flight Initiation – Takeoff: Each UAV is transported to its starting point and takes off.
   - Data Acquisition: Upon reaching the desired altitude, each UAV begins collecting images of the crop.
   - Data Forwarding: Each image is immediately forwarded to the ground workstation via the FANET and ground network.
   - Flight Termination – Landing: Each UAV lands at a predefined point upon mission completion.
3) Post-Flight Data Exploration Stage:
   - Data Exploitation: The image data are directly processed using software that merges the images based on geolocation information to create a single mosaic image illustrating the entire surveyed area.
   - Results: The mosaic along with other types of images, are analyzed and used by stakeholders for reference and decision-making.

This FANET-based approach significantly enhances efficiency, reduces mission time, minimizes manual intervention, and mitigates the risk of mission failure due to the distributed nature of the UAV network.

Fig. (4) shows the simulated agricultural field to be surveyed. Assuming an area of interest measuring $1000m \times 1000m$, and considering that a UAV can capture a snapshot of $50m \times 50m$ from a height (h), the side-step size can be configured as 50m, enabling the complete coverage of the area in 19 vertical sweeps. The UAV transmits these snapshots to a ground workstation (sink), as illustrated in Fig. (4), positioned at the bottom right corner of the field. With the UAV cruising at a speed of 20m/s [43], the entire operation can be finalized within approximately 17 minutes ($19.900m/20m/s = 995$ seconds).

This research encompasses the deployment of up to 5 drones. The simulated drone, showcased in Fig. (5), maintains a consistent altitude of 10 meters above ground level throughout its flight trajectory. Static ground nodes, facilitating communication among themselves and with the aerial nodes, provide support for the FANET. The agricultural field accommodates 25 ground static nodes, arranged in a $5 \times 5$ grid configuration, as shown in Fig. (5). Additionally, the cabin house located in the lower right corner of the field, as depicted in Fig. (5), functions as the sink node.

Considering the UAVs' velocity of 20m/s, each would capture 20 images during a sweep covering 1000m, resulting in an image capture rate of approximately one every 2.5 seconds. Assuming a compressed image size of 1 MB, the UAVs would need to transmit 1 MB of data every 2.5 seconds. However, transmission is scheduled once every 5 seconds, necessitating each node to transmit a minimum of 2 MB of data within this interval, corresponding to a transmission rate of at least 0.5 Mbps.

It's worth noting that a higher on-time would augment the transmission rate but concurrently escalate network overhead. To optimize overall performance, a judicious on-time and off-time window should be established. With these considerations in mind, the MAC channel should support a minimum of 0.5 Mbps. However, conventional PHY / MAC IEEE802.11b exhibits rates below 500 kbps due to congestion in typical MANET, and FANET scenarios. To address this limitation, a higher-capacity PHY / MAC, such as IEEE802.11n, is adopted for the FANET scenario, boasting enhanced data rates and a communication range exceeding 400 meters in open outdoor settings [44].

The simulation scenario will employ AERO-FL for comparative analysis alongside three well-established routing protocols in ad hoc networks: AODV, OLSR, and DSDV.

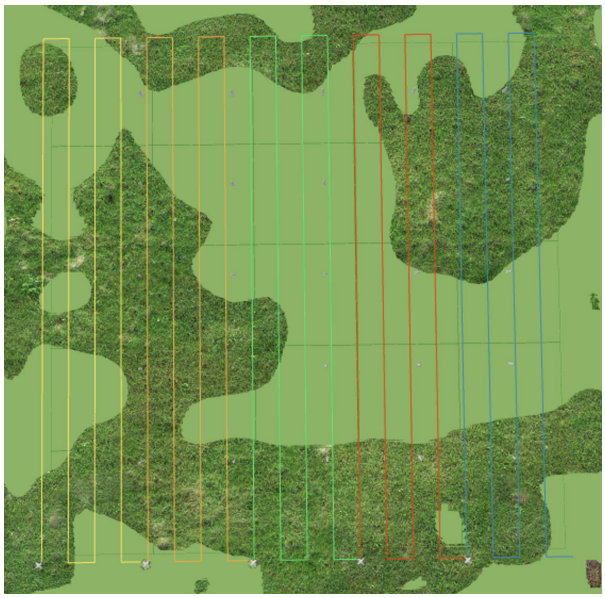

**FIGURE 4.** FANET simulation scenario, each UAV area of coverage has a different color.

**FIGURE 5.** Close-up view of UAVs in the foreground, ground nodes in the background, and the cabin house on the right side of the field.

Originally devised for MANETs [45], AODV has exhibited notable effectiveness within FANETs, consistently achieving high packet delivery ratio, particularly in scenarios employing stochastic mobility models [16]. The adaptability of AODV is highlighted by the emergence of several FANET-specific protocols rooted in its principles, underscoring its ability to address mobility patterns characterized by randomness [46].

### A. NETWORK PERFORMANCE METRICS

The scenario employs a set of metrics to assess and compare the performance of the proposed routing protocol. These metrics were carefully chosen to provide a comprehensive evaluation of the models and to enable a thorough analysis of their respective capabilities.

1) Packet delivery ratio, expressed as a percentage, stands as a pivotal performance metric delineating the fraction of packets successfully conveyed from their source to the intended destination within a communication network. It serves as a paramount gauge of the overall efficiency and dependability of a network protocol or system. packet delivery ratio computation entails dividing the total number of packets received at the destination by the aggregate number of packets transmitted from the source.

$$PacketDeliveryRatio(\%) = \frac{Sink_{received}}{Sender_{sent}}\ x\ 100 \quad (3)$$

The measurement of packet delivery ratio furnishes researchers with invaluable insights into the effectiveness and resilience of the network, enabling them to gauge the caliber and success rate of packet delivery, which constitutes a cornerstone for assessing and fine-tuning network performance.

2) Cumulative delay at the destination node constitutes a metric encapsulating the temporal differential between packet arrival at the sink node and its transmission from the source to the sink. This metric quantifies the comprehensive delay experienced by packets during their traversal through the network. Typically gauged in milliseconds (ms), it denotes the accrued time taken for packets to reach their designated endpoint. The mathematical formula for calculating cumulative delay typically involves summing up the individual delays experienced by packets as they traverse through network.

$$D_{cumulative} = D_1 + D_2 + D_3 + \ldots + D_n \quad (4)$$

where $D_1$, $D_2$, $D_3$, $D_n$ represent the individual delays experienced by each packet at different stages or network components during its journey from the source to the destination, and n represents the total number of network components or stages that the packet traverses. Cumulative delay at the destination confers invaluable insights into the efficacy and performance of the network, aiding researchers and network administrators in evaluating the efficacy of routing protocols and identifying potential bottlenecks or latencies. Through the analysis of this metric, one can assess the repercussions of network conditions and congestion on the overall delivery time of packets. Diminished cumulative delays denote swifter and more efficient transmission, pivotal for applications necessitating prompt data delivery.

3) Average Energy Consumption of a Network pertains to the collective energy utilization across all network entities within a defined timeframe. This metric encompasses the energy outlay associated with diverse network elements, as they operate within the network infrastructure. From a research perspective, quantifying the average energy consumption of a network is pivotal for assessing its overall energy efficiency and environmental sustainability. This metric sheds light on the power consumption of network components during essential operations like data transmission, reception, routing, and processing. To gauge the average energy consumption of a network, each network component's energy usage is measured independently, with the cumulative sum representing the network's aggregate energy consumption, divided by the total number of network components. Mathematically, the total energy consumption in a network can be described as:

$$Energy_{average} = \frac{\sum_{i=1}^{n} E_i\ x\ t}{n} \quad (5)$$

where $E_i$ represents the energy consumption rate of the $i^{th}$ network component measured in units such as Watts (W) or Joules (J) per second, t represents the duration of operation or simulation time, and n represents the total number of network components. Thorough comprehension and analysis of a network's total energy consumption are imperative for network designers, administrators, and researchers. It enables the development of strategies aimed at optimizing energy utilization, reducing environmental impact, and bolstering overall network performance and sustainability.

4) Normalized Energy Consumption (NEC) is a custom metric designed to provide insights into the energy efficiency of individual network nodes relative to their achieved packet delivery ratio. This metric offers a normalized perspective on energy consumption, considering the energy expenditure of nodes in relation to their effectiveness in packet delivery. Mathematically, NEC is defined as the average energy consumption of a node divided by its corresponding packet delivery ratio. This ratio allows for a direct comparison between the energy consumed by a node and its performance in delivering packets successfully.

$$NEC = \frac{NodeAverageEnergyConsumption}{PacketDeliveryRatio} \quad (6)$$

The numerator represents the average energy consumption of a node, encompassing the energy utilized during various network activities such as data transmission, reception, and processing. The denominator, packet delivery ratio, signifies the node's effectiveness in delivering packets, quantifying the proportion of successfully delivered packets relative to those transmitted. By normalizing energy consumption against packet delivery ratio, this metric enables a more comprehensive assessment of a node's energy efficiency. A lower value of the Normalized Energy Consumption (Ratio) indicates that the node achieves a higher packet delivery ratio relative to its energy consumption, reflecting greater energy efficiency and network performance optimization.

5) Number of Forwards of Data Packets refers to the count of times a data packet is forwarded by intermediate nodes within a network before reaching its final destination. The Number of Forwards of Data Packets is a metric used to quantify the extent of packet forwarding activity within a network. It provides valuable insights into the routing behavior and efficiency of the network, reflecting the complexity and robustness of the routing paths traversed by data packets. This metric is particularly relevant in evaluating the performance and reliability of routing protocols, as it indicates the level of network congestion, packet loss, and routing overhead experienced during data transmission. A higher number of forwards of data packets may signify suboptimal routing paths, network bottlenecks, or excessive packet retransmissions, all of which can impact network latency, throughput, and overall performance.

Through the utilization of these metrics, the objective of this paper is to delve into the distinctive attributes and limitations inherent in each routing protocol. Furthermore, it seeks to evaluate the efficacy of the proposed routing protocol in confronting the intricacies of a deterministic UAV operation, thereby providing a comprehensive understanding of its performance in practical scenarios.

Table (2) presents the simulation parameter values for the investigated scenario.

**TABLE 2. Simulation parameter values for smart farming scenario.**

| Parameter | Value |
|---|---|
| Simulation area | 1000m x 1000m |
| Side-step | 50m |
| UAVs' type | Multicopters |
| UAVs' speed | 20 m/s |
| Height of the flight | 10m |
| Pause Time | 2 sec |
| Routing Protocols | OLSR<br>AODV<br>DSDV<br>AERO-FL |
| Number of UAVs | 1,2,3,4,5 |
| Number of Sink Nodes | 1 |
| Mobility Model | 3D Capable Deterministic Scan |
| PHY / MAC | 802.11n |
| Packet Size | 512 Bytes |
| Traffic Rate | 5 Mbps |
| Traffic Type | 5 On/Off |
| Traffic (On-Time) | 2.5 seconds |
| Traffic (Off-Time) | 2.5 seconds |

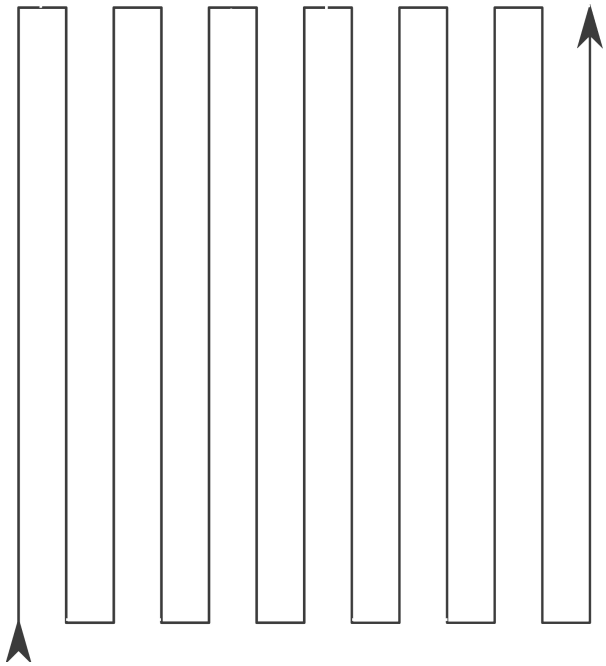

**FIGURE 6. The scanning path of the UAV presented in a 2D space.**

## VI. MOBILITY MODEL

Fig. (6) illustrates the scanning path of the UAV, considering that the UAV flies at a constant given height, following the curvature of the ground.

The proposed 3D scan mobility model is beneficial in these real-world applications by offering a closer approximation of UAV movements, improving the effectiveness and realism of simulations.

### A. MOVEMENTS OF SCANNING MOBILITY

#### 1) THE VELOCITY VECTOR

The velocity vector is a vector quantity that represents the rate at which an object changes its position. It is defined as the derivative of the position vector with respect to time:

$$v = dr/dt \tag{7}$$

where $v$ is the velocity vector, $r$ is the position vector, $t$ is time. In component form, the velocity vector can be expressed as:

$$v = (v_x + v_y + v_z) \tag{8}$$

where, $v_x$, $v_y$ and $v_z$ are the components of the velocity vector in the $x$, $y$, and $z$ directions, respectively.

#### 2) THE VERTICAL AND HORIZONTAL MOVEMENT

The following equation shows the vertical velocity $v_v$:

$$v_v = (\cos\theta \times \sin\phi \times s, \sin\theta \times \sin\phi \times s, \cos\phi \times s) \tag{9}$$

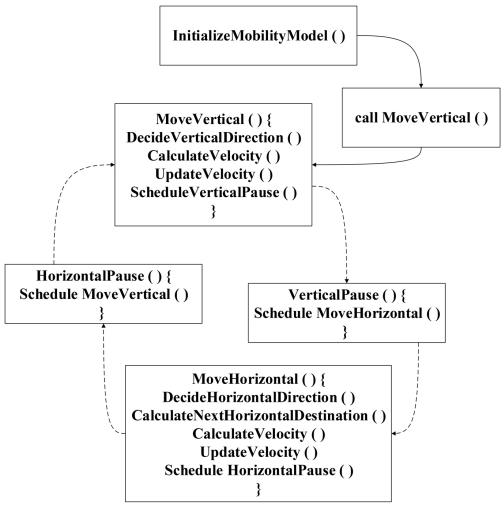


**FIGURE 7.** The flow chart of 3D scan mobility model.

where $\theta$ is the angle of vertical direction, and may have value $\pi/2$ or -$\pi/2$ to represent the top and bottom direction of the motion. $\phi$ is the pitch to represent the motion in z direction and it may also have value $\pi/2$ or -$\pi/2$ to represent the up and down direction of motion. S is the scalar that represents speed.

The following equation shows the horizontal velocity $v_h$:

$$v_h = (\cos\phi \times \sin\phi \times s, \sin\phi \times s, \cos\phi \times s) \tag{10}$$

where $\phi$ is the angle of horizontal direction, and may have value 0 or $\pi$ to represent the left and right direction of the motion.

### B. FLOW DIAGRAM OF 3D SCAN MOBILITY MODEL

The following flow diagram explains the overall design of the proposed 3D Scan Mobility Model.

In Fig. (7), the dashed lines depict the control flow that is slated for processing at a predefined future time. As such, the established mobility pattern persists in the same trajectory until that specific moment. Subsequently, at the scheduled time, an alteration in course transpires after a brief pause. Consequently, the ensuing movement direction hinges upon the functions associated with the upcoming scheduled event. This pattern endures until the conclusion of the simulation time frame.

### C. PSEUDO CODE OF THE ALGORITHM

Algorithm (1) explains the algorithm of the 3D Scan mobility model:

Algorithm (1) expects the following inputs: $X_{min}$, $X_{max}$, $Y_{min}$, $Y_{max}$, $\theta$, $\phi$, s, d

Where

$X_{min}$, $X_{max}$, $Y_{min}$, $Y_{max}$ : the bounds of the region,

$\theta$ : the angle of vertical direction; $2\pi$ or - $2\pi$,

$\phi$ : the angle of horizontal direction; $\pi$ or 0,

s: speed of the object,

**Algorithm 1** 3D Scan Mobility Model

**procedure** MoveVertical
  $P_{\text{Current}} \leftarrow$ MobilityModelGetPosition()
  **if** $P_{\text{next}}(y) > Y_{\max} or P_{\text{next}}(y) < Y_{\min}$ **then**
    $\theta \leftarrow -\theta$
  **end if**
  $v_v \leftarrow (\cos\theta \cdot \sin\phi \cdot s, \sin\theta \cdot \sin\phi \cdot s, \cos\phi \cdot s)$
  MobilityModelSetVelocity($v_v$)
  UnpauseMobility()
  $distance \leftarrow Y_{\max} - Y_{\min}$
  $delay \leftarrow \frac{distance}{s}$
  ScheduleEvent($delay$, VerticalPause())
**end procedure**
**procedure** MoveHorizontal
  $P_{\text{Current}} \leftarrow$ MobilityModelGetPosition()
  $P_{\text{next}} \leftarrow P_{\text{Current}}$
  $P_{\text{next}}(x) \leftarrow P_{\text{next}}(x) + d$
  **if** $P_{\text{next}}(x) > X_{\max} or P_{\text{next}}(x) < X_{\min}$ **then**
    $d \leftarrow -d$
    **if** $\theta == 0$ **then**
      $\theta \leftarrow \pi$
    **else**
      $\theta \leftarrow 0$
      $P_{\text{next}}(x) \leftarrow P_{\text{next}}(x) - \frac{d}{2}$
    **end if**
  **end if**
  $v_h \leftarrow (\cos\phi \cdot \sin\phi \cdot s, \sin\phi \cdot \sin\phi \cdot s, \cos\phi \cdot s)$
  MobilityModelSetVelocity($v_h$)
  $distance \leftarrow |P_{\text{Current}} - P_{\text{next}}|$
  $delay \leftarrow$ Seconds $\left(\frac{distance}{s}\right)$
  ScheduleEvent($delay$, HorizontalPause())
**end procedure**
**procedure** VerticalPause
  ScheduleEvent(pause, MoveHorizontal())
**end procedure**
**procedure** HorizontalPause
  ScheduleEvent(pause, MoveVertical())
**end procedure**

### D. IMPLEMENTATION OF 3D SCAN MOBILITY MODEL UNDER NS-3

The proposed mobility model and the respective simulations were carried out using 3 tools: ns-3 [47], NetSimulyzer 3D Visualization Tool and NetSimulyzer ns-3 module [48]. Ns-3 is a discrete-event network simulator designed for Internet systems and serves as a tool for researchers and developers to explore, simulate, and assess network protocols, applications, and services within a controlled environment. It is important to note that ns-3 employs the Cartesian coordinate system, denoted as (x, y, z), while the proposed mobility model utilizes the spherical coordinate system, defined by (r, $\theta$, $\phi$). In this context, the radius 'r' can be interpreted as $v$ when referring to speed. A visual representation of these coordinate systems is provided in Fig. (8).

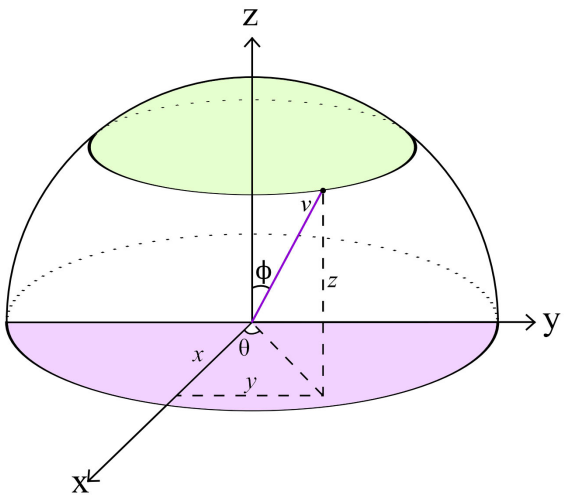


**FIGURE 8.** ns-3 Cartesian coordinate system denoted as (x, y, z), and mobility models spherical coordinate system denoted as ($r$, $\theta$, $\phi$).

Recognizing the advantages of its enhanced functionality and improved performance, the proposed mobility model is implemented using ns-3 version 3.37. This decision helped to leverage the latest add-on offered by the simulator, such as NetSimulyzer.

NetSimulyzer is a versatile 3D visualization tool, that offers a comprehensive solution for showcasing, troubleshooting, delivering presentations, and comprehending ns-3 scenarios. Given the limitations of NetAnim, the default visualization tool in ns-3, in depicting network scenarios in 3D, the decision was made to utilize NetSimulyzer to enhance the visualization and comprehension of the proposed 3D network scenario. This choice facilitates a superior visualization experience, enabling a more thorough understanding of the intricate network dynamics and interactions within the simulated environment.

Fig. (9) depicts the simulation of a dynamic 3D scenario utilizing the 3D Scan mobility model, which has been visually rendered using the advanced NetSimulyzer 3D visualization tool. The figure showcases the immersive representation of the network's mobility patterns, offering a comprehensive and visually captivating view of the simulated environment.

## VII. AERO-FL ROUTING PROTOCOL

Drawing from the literature review in Section (II), various factors could potentially impede the effective deployment of a routing protocol within a deterministic scenario akin to the network model outlined in Section (V). These factors encompass a range of considerations, including but not limited to:

1) High Mobility of Fast-Moving Drones: The rapid movement of drones leads to frequent link failures, disrupting communication paths.
2) Redundant Hello Messages from Static Nodes: Static nodes in the network redundantly broadcast hello messages, even when their locations remain unchanged, resulting in unnecessary overhead.

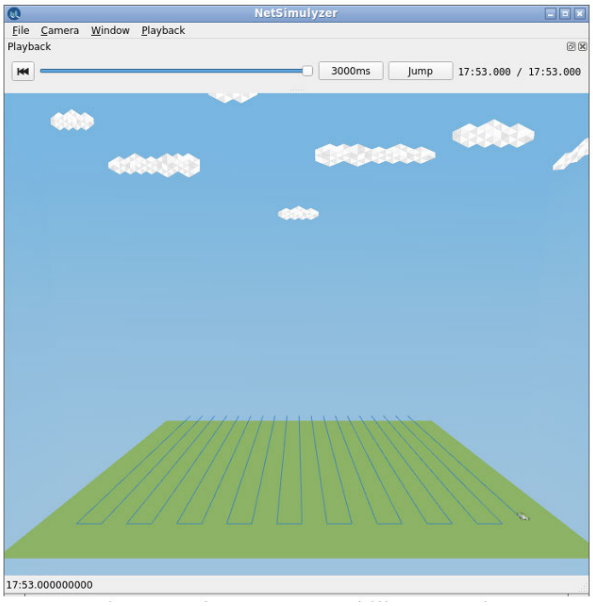


**FIGURE 9.** The 3D Scan mobility model using NetSimulyzer add-on.

3) Uniform Hello Message Transmission Rates: Both fast-moving drones and static nodes transmit hello messages at the same rate, regardless of their mobility or network topology.
4) Sparse and Dense Regions: Ad hoc network in agricultural scenarios often encompass vast areas with variations in node density, leading to regions with sparse or dense node distribution.
5) Variability in 1-Hop Connectivity: 1-hop connectivity refers to the number of neighboring UAVs within direct communication range that a node can use to forward data. Drones positioned at the central part of the network may enjoy better 1-hop connectivity compared to those situated at the network periphery.

To address these issues and enhance performance in an air-to-ground communication, two main strategies are proposed:

1) Optimization of Hello Interval: Adjusting the hello interval to reduce overall message overhead and minimize redundant hello message transmissions.
2) Improvement of 1-Hop Connectivity: Enhancing the 1-hop connectivity of all nodes, both mobile and static, to establish more robust communication links within the network.

Improving 1-hop connectivity involves increasing the transmission power of nodes, although determining the optimal power level presents a challenge. Increasing transmission power escalates overhead and energy consumption. To mitigate these effects, we adopt a nuanced approach by incrementally adjusting transmission power based on the node's current 1-hop connectivity or approximate network density.

Nodes employ fuzzy logic to dynamically select transmission power levels from three options (low, medium, high), with the default power level set as the starting point. This

adaptive strategy ensures that nodes adjust their transmission power slightly according to their current connectivity status, thereby reducing link failures and enhancing overall network performance.

It is crucial to acknowledge that while optimizing transmission power enhances 1-hop connectivity and improves performance metrics such as packet delivery ratio, it also leads to increased overall energy consumption. The goal of this approach is to achieve superior performance in these metrics without disproportionately escalating power consumption. Therefore, the proposed optimization strategy seeks to minimize the power consumption per unit of packet delivery ratio, thereby ensuring efficient and sustainable overall network performance.

### A. FUZZYFICATION IN OUR DESIGN

Fuzzification is a technique through which the 'crisp-valued' inputs are converted into fuzzy-valued outputs. The following are the things needed to understand the fuzzification process.

#### 1) LINGUISTIC VARIABLES

In fuzzy logic, Linguistic Variables (LV) are variables whose values are words or phrases rather than numerical values. These variables allow for more natural and intuitive representation of uncertainty and imprecision in human language. In our design, we used 'high', 'medium' and 'low' as three Linguistic variables in our model to make decision-making processes, where the uncertainty of the input data can be represented more accurately using fuzzy logic.

#### 2) INPUT, OUTPUT VARIABLES AND MEMBERSHIP FUNCTIONS

The following are the three input membership functions used in the proposed design. The variable on the left is called input membership variable.

$$MF_{in} = \begin{cases} 1 - hopConnectivity: & \{\text{Low, Medium, High}\} \\ CurrentTxPower: & \{\text{Low, Medium, High}\} \\ PrevHelloInterval: & \{\text{Low, Medium, High}\} \end{cases} \tag{11}$$

The following are the three output membership functions used in the proposed design. The variable on the left is called output membership variable.

$$MF_{out} = \begin{cases} NewTxPower: & \{\text{Low, Medium, High}\} \\ NewHelloIntval - S: & \{\text{Low, Medium, High}\} \\ NewHelloIntval - M: & \{\text{Low, Medium, High}\} \end{cases} \tag{12}$$

where NewHelloIntval-S is the hello interval that will be set on static/non-mobile nodes of the FANET and the NewHelloIntval-M is the hello interval that will be set on mobile drone nodes.

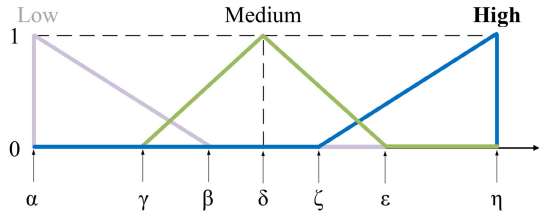


**FIGURE 10.** Membership diagram representing an input / output membership function.

#### 3) MEMBERSHIP DIAGRAM

The following membership diagram demonstrates the concept of a triangular membership function. In this diagram, both the input and output membership functions are similar in appearance, as they utilize the same linguistic variables for the three input membership functions and the three output membership functions. The triangular shapes across all six functions are identical. The primary difference lies in the values $\alpha$ to $\eta$, which denote varying ranges within the input and output functions. Fig. (10) illustrates all six input and output membership functions.

The primary objective is to adjust the values of output variables in response to input variables based on fuzzy logic rules. One-hop connectivity is determined by the number of neighbors within one hop that are detected by a node through overhearing hello messages periodically transmitted from those neighboring nodes. This can be considered as the realized neighbor density at a given time. It is important to note that the actual number of physical neighbors may vary, hence the term ''1-hop connectivity'' is used to refer to successfully connectable neighbors. Theoretically, an increase in 1-hop connectivity indicates better overall connectivity.

1-hop connectivity can be improved by increasing the transmission Tx power of the nodes. However, this also results in increased overhead and power consumption. Therefore, determining the optimal Tx power is crucial for achieving balanced performance. Ideally, if the 1-hop connectivity reaches an optimal range, it can be considered good connectivity. For instance, if the 1-hop connectivity is below this optimal range, the Tx power needs to be increased, but the exact increment required is uncertain. Conversely, if the 1-hop connectivity exceeds the optimal range, the Tx power should be decreased, yet the precise reduction needed is also uncertain. Fuzzy logic provides a solution to these uncertainties by determining the appropriate adjustments to the Tx power, ensuring optimal performance.

#### 4) RANGE OF VALUES

Table (3) shows an example of range of values that one may use to take decision based on fuzzy logic.

#### 5) TRIANGLE MEMBERSHIP FUNCTIONS

Triangular membership functions are employed to delineate the range of input variables in our fuzzy system. To avoid redundancy, a single set of triangular membership functions is

**TABLE 3.** The input and output variables and their range.

| | Variable | Low | | Medium | | | High | |
|---|---|---|---|---|---|---|---|---|
| | | $\alpha$ | $\beta$ | $\gamma$ | $\delta$ | $\epsilon$ | $\zeta$ | $\eta$ |
| Inputs | 1-hopConnectivity | 0 | 8 | 5 | 15 | 20 | 15 | 25 |
| | CurrentTxPower | 10 | 15 | 13 | 20 | 25 | 20 | 30 |
| | PrevHelloIntVal | 1 | 2 | 1.5 | 3 | 4 | 3.5 | 5 |
| Outputs | NewTxPower | 10 | 13 | 12 | 15 | 18 | 17 | 20 |
| | NewHelloIntVal-S | 2 | 3 | 2.5 | 4 | 6 | 5 | 8 |
| | NewHelloIntVal-M | 1 | 2 | 1.5 | 2.5 | 3 | 2.5 | 4 |

illustrated, representing the general concept. In practice, each set of triangular functions may span different value ranges for the parameters $\alpha$ to $\eta$. The following explanation covers the three membership functions that define 'low,' 'medium,' and 'high' values. It is important to note that the actual value ranges may vary depending on the specific input and output variables presented in Table (3). The function provided below pertains to the left triangle in the example membership diagram.

$$\mu_{low}(x) = \begin{cases} 0, & \text{for x} < \alpha \\ 1, & \text{for x} = \alpha \\ \dfrac{x-\alpha}{\beta-\alpha}, & \text{for } \alpha < \text{x} < \beta \\ 0, & \text{for x} \geq \beta \end{cases} \tag{13}$$

The following function belongs to the middle triangle of the above example membership diagram.

$$\mu_{medium}(x) = \begin{cases} 0, & \text{for x} \leq \gamma \\ \dfrac{x-\gamma}{\delta-\gamma}, & \text{for } \gamma < \text{x} < \delta \\ \dfrac{x-\delta}{\epsilon-\delta}, & \text{for } \delta < \text{x} < \epsilon \\ 0, & \text{for x} \geq \epsilon \end{cases} \tag{14}$$

The following function belongs to the right triangle of the above example membership diagram.

$$\mu_{high}(x) = \begin{cases} 0, & \text{for x} \leq \zeta \\ \dfrac{x-\alpha}{\beta-\alpha}, & \text{for } \alpha < \text{x} < \beta \\ 1, & \text{for x} = \zeta \\ 0, & \text{for x} \geq \zeta \end{cases} \tag{15}$$

### B. FUZZY SET OPERATIONS

Fuzzy set operations are integral to the fuzzy logic mechanism, as they determine how a value within a range is actually decided. Evaluating fuzzy rules and combining the results of individual rules are executed through these operations. It is important to note that operations on fuzzy sets differ from those on non-fuzzy sets. Let $\mu_A$, $\mu_B$, and $\mu_C$ represent the membership functions for fuzzy sets $A$, $B$, and $C$ of different input variables. For a given set of crisp inputs, these membership functions return different confidence values based on their nature. In order to integrate the outputs of these membership functions, various techniques are applied. The most commonly used operations for OR and AND operators

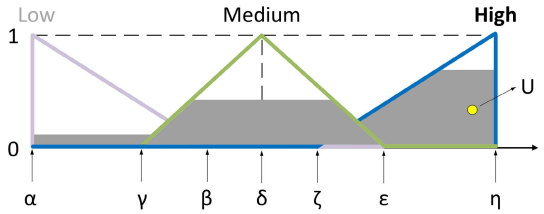


**FIGURE 11.** Defuzzification from an output membership function.

are the maximum and minimum, respectively. The following equations illustrate these operations:

$$MAX : Max\{\mu A(x), \mu B(x), \mu C(x)\} \tag{16}$$

$$MIN : Min\{\mu A(x), \mu B(x), \mu C(x)\} \tag{17}$$

The purpose of this operation is to determine the value of an input or output variable based on three distinct membership functions. When a complement (NOT) operation is required for a single input, the following equation is applied to the fuzzy set:

$$NOT : \mu A(x) = 1 - \mu A(x) \tag{18}$$

After evaluating the outcome of each rule, these results need to be aggregated to derive a final conclusion. This process, known as inference, can be performed using various methods. The following are some of the common accumulation techniques used to combine the outcomes of individual rules:

$$Maximum : Max\{\mu A(x), \mu B(x), \mu C(x)\} \tag{19}$$

$$BoundedSum : Min\{1, \mu A(x) + \mu B(x), \mu C(x)\} \tag{20}$$

$$NormalizedSum : \frac{\mu A(x) + \mu B(x) + \mu C(x)}{Max\{1, Max\{\mu A(x_0), \mu B(x_0), \mu B(x)\}\}} \tag{21}$$

The maximum algorithm is used for accumulation.

### C. DEFUZZIFICATION

The defuzzification stage involves converting the fuzzy outputs of different variables from the inference stage into crisp values, achieved through a defuzzifier. This process is conducted based on the membership function of the output variable. For instance, Fig. (11) illustrates the result at the end of the inference process. In this figure, the shaded areas represent the fuzzy outcome. The goal of defuzzification is to extract a crisp value, indicated by a dot in the figure, from this fuzzy result.

Various algorithms are employed for defuzzification, with the center of gravity method being one of the most commonly used. This method integrates all the individual fuzzy outputs to produce a single (or sometimes multiple) crisp output. The center of gravity, or centroid, is determined using the following integration formula to compute the value of U:

$$U = \frac{\int_{min}^{max} u\mu(u)\,du}{\int_{min}^{max} \mu(u)\,du} \tag{22}$$

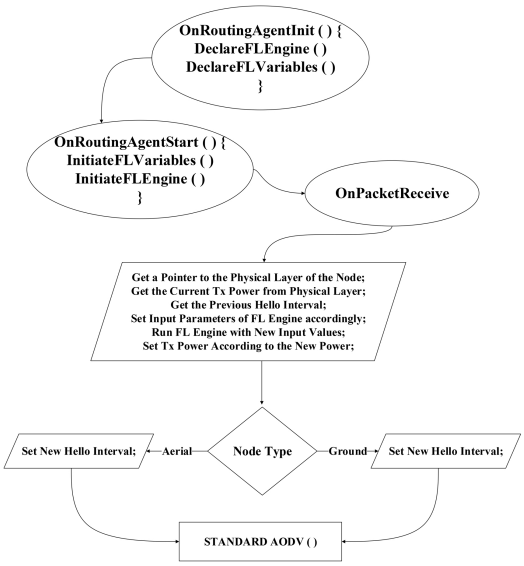


**FIGURE 12.** The flow diagram of AERO-FL.

It is important to note that if multiple crisp outputs are required, multiple center of gravity calculations will be necessary. In our scenario, we need to obtain three crisp outputs from our three output variables.

### D. THE FLOW DIAGRAM OF AERO-FL

Fig. (12) presents the idea of integration of fuzzy logic inside the standard AODV design.

At the beginning of the process, the agent responsible for protocol initialization defines and initializes the fuzzy logic engine along with the relevant variables. When a new packet is received, the algorithm retrieves values for transmission power, and message intervals which are used as inputs in the fuzzy system. Based on the node type, the fuzzy system selects the updated message intervals from the proposed outputs. The remaining steps in the algorithm adhere to the principles of traditional AODV protocol.

### E. THE PSEUDO CODE OF AERO-FL

AERO-FL builds upon the foundational principles and core functionalities of the AODV routing protocol. In standard AODV, the transmission power and hello intervals remain static and are not dynamically adjusted based on network parameters. However, in the proposed fuzzy logic-based adaptation of AODV, these two parameters are optimized over time concerning one-hop connectivity and the previously used transmission power. The following pseudo-code illustrates the specific section of the AODV algorithm where this optimization technique is integrated, transforming it into AERO-FL. It is important to note that, aside from this enhancement, the other functions of AERO-FL remain identical to those of AODV, and thus they are not detailed in this pseudo-code.

Algorithm (2) explains the algorithm of the AERO-FL Routing Protocol:

**Algorithm 2** AERO-FL Routing Protocol

```
OnAeroFLInit() {
  FLEngine ← NewFLEngine();
  CurrentTxPower ← InputVariable(α1, β1, γ1, δ1, ϵ1, ζ1, η1);
  1hopConnectivity ← InputVariable(α2, β2, γ2, δ2, ϵ2, ζ2, η2);
  PrevHelloIntVal ← InputVariable(α3, β3, γ3, δ3, ϵ3, ζ3, η3);
  NewTxPower ← OutputVariable(α4, β4, γ4, δ4, ϵ4, ζ4, η4);
  NewHelloIntValS ← OutputVariable(α5, β5, γ5, δ5, ϵ5, ζ5, η5);   ▷ For Static Nodes
  NewHelloIntValM ← OutputVariable(α6, β6, γ6, δ6, ϵ6, ζ6, η6);   ▷ For Mobile Nodes
  FLEngine− > addInputVariable(CurrentTxPower);
  FLEngine− > addInputVariable(1hopConnectivity);
  FLEngine− > addInputVariable(PrevHelloIntVal);
  FLEngine− > addOutputVariable(NewTxPower);
  FLEngine− > addOutputVariable(NewHelloIntValS);
  FLRulesInisialized = false;
}
OnReceiveAeroFL(Packet) {
  FLEngine ← NewFLEngine();
if (OptimisationType == 1) then
    node ← GetObject(this);                          ▷ Get Current Node
    dev ← GetDevice(node, 0);                        ▷ Get 0th Device of the Node
    phy ← GetPhy(dev);                               ▷ Get Physical Layer of the Device
    FLEngine− > setInputValue(PrevHelloIntVal, mHelloIntVal);
    FLEngine− > setInputValue(1hopConnectivity, mnb.count);
    FLEngine− > setInputValue(CurrentTxPower, Phy.GetTxP());
    FLEngine− > process();
    NewTxP ← FLengine− > getOutputValue("NewTxPower");
    if (Ntype == 3) then                             ▷ 0-default, 1-sink, 2-Static Node, 3-UAV
      SetHelloInt(FLEngine− > getOutputValue(NewHelloIntValM));
    else
      SetHelloInt(FLEngine− > getOutputValue(NewHelloIntValS));
    end if
end if
}
OnAeroFLStart() {
if (!FLRulesInitialized) then
    DefineTxPowerRules();
    DefineHelloIntervalRulesForStaticNodes();
    DefineHelloIntervalRulesForMobileNodes();
    FlRulesInisialized = true;
end if
}
```

Algorithm (2) expects the following inputs for the input membership function

- Index 1: $(\alpha_1, \beta_1, \gamma_1, \delta_1, \epsilon_1, \zeta_1, \eta_1)$ stands for 1 hop Connectivity
- Index 2: $(\alpha_2, \beta_2, \gamma_2, \delta_2, \epsilon_2, \zeta_2, \eta_2)$ stands for Current Tx Power
- Index 3: $(\alpha_3, \beta_3, \gamma_3, \delta_3, \epsilon_3, \zeta_3, \eta_3)$ stands for PrevHelloIntVal

Algorithm (2) expects the following inputs for the output membership function

- Index 4: $(\alpha_4, \beta_4, \gamma_4, \delta_4, \epsilon_4, \zeta_4, \eta_4)$ stands for NewTxPower
- Index 5: $(\alpha_5, \beta_5, \gamma_5, \delta_5, \epsilon_5, \zeta_5, \eta_5)$ stands for NewHelloIntVal -S
- Index 6: $(\alpha_6, \beta_6, \gamma_6, \delta_6, \epsilon_6, \zeta_6, \eta_6)$ stands for NewHelloIntVal -M

and Node Type.

Where the above sets define the ranges of three input triangular functions and 3 output triangular functions, and node type stands for the type of node that takes the following values: 0-default, 1-sink, 2-static, 3-UAV.

The fuzzy logic rules provide a framework for dynamically adjusting a node's transmission power and hello message interval for static and mobile nodes, based on its 1-hop connectivity and current transmission power state. These rules aim to optimize energy efficiency while maintaining reliable communication across the network. Algorithm (3) processes two key inputs: the current transmission power (CurrentTxPower) and 1-hop connectivity, which are both represented across three fuzzy categories: Low, Medium, and High. Based on these inputs, the algorithm determines the new transmission power level, the hello message interval for static nodes, and the hello message interval for mobile nodes. By applying the defined fuzzy rules, on the one hand the system adapts transmission power in response to network conditions, reducing power when 1-hop connectivity is high and increasing it when connectivity is low, always accounting for the current power level to ensure a balanced approach, and on the other hand, the system adapts hello message interval in response 1-hop connectivity, increasing the interval when 1-hop connectivity is high and decreasing it when connectivity is low.

### F. NS-3 IMPLEMENTATION

In addition to the simulation and visualization tools introduced in Section (V), Fuzzylite, an open-source fuzzy logic control library programmed in C++ for multiple platforms, is integrated. The Fuzzylite Libraries offer a seamless approach to designing and operating fuzzy logic controllers within an object-oriented programming paradigm. Unlike many other fuzzy logic libraries, Fuzzylite is lightweight and does not rely on external dependencies, making it an ideal choice for computationally constrained environments or real-time applications. Moreover, Fuzzylite offers extensive customization options for defining fuzzy inference systems, including the ability to create complex rule sets, specify membership functions, and apply defuzzification methods. This flexibility makes it particularly suitable for optimizing routing decisions in the proposed FANET scenario.

## VIII. NUMERICAL RESULTS

This section presents a comprehensive analysis of the performance evaluation performed on the proposed routing protocol against three well-established protocols in ad hoc networks. This evaluation encompasses five key metrics packet delivery ratio, cumulative delay, average energy consumption per node, normalized energy consumption per node, and hop count. Each metric offers valuable information on the efficiency, reliability, and overall effectiveness of the routing protocols under examination.

**Algorithm 3** Fuzzy Logic Rules for AERO-FL Routing Protocol

```
DefineTxPowerRules() { ▷ Power Transmission Rules
if (CurrentTxPower == High) ∧ (1hopConnectivity == High) then
    NewTxPower ← Medium
end if
if (CurrentTxPower == Medium) ∧ (1hopConnectivity == High) then
    NewTxPower ← Low
end if
if (CurrentTxPower == Low) ∧ (1hopConnectivity == High) then
    NewTxPower ← Low
end if
FLengine− > AddRule(TxPRule);
}
DefineHelloIntValRulesForStaticNodes() { ▷ Hello Interval Rules for Static Nodes
if (1hopConnectivity == High) then
    NewHelloIntValS ← High
end if
if (1hopConnectivity == Medium) then
    NewHelloIntValS ← Medium
end if
if (1hopConnectivity == Low) then
    NewHelloIntValS ← Low
end if
FLengine− > AddRule(NewHelloIntValS);
}
DefineHelloIntValRulesForMobileNodes() { Hello Interval Rules for Mobile Nodes
if (1hopConnectivity == High) then
    NewHelloIntValM ← High
end if
if (1hopConnectivity == Medium) then
    NewHelloIntValM ← Medium
end if
if (1hopConnectivity == Low) then
    NewHelloIntValM ← Low
end if
FLengine− > AddRule(NewHelloIntValM);
}
```

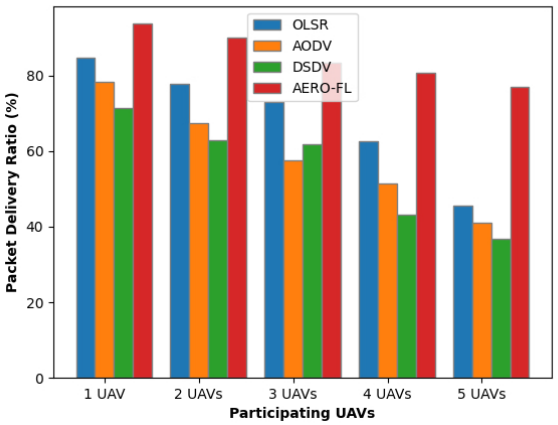


**FIGURE 13.** Performance of the application layer in terms of packet delivery ratio.

### A. PACKET DELIVERY RATIO

Fig. (13) presents the packet delivery ratio associated with each routing protocol.

When the network consists of a single UAV, all protocols achieve relatively high packet delivery ratios. AERO-FL emerges as the top performer, achieving a packet delivery

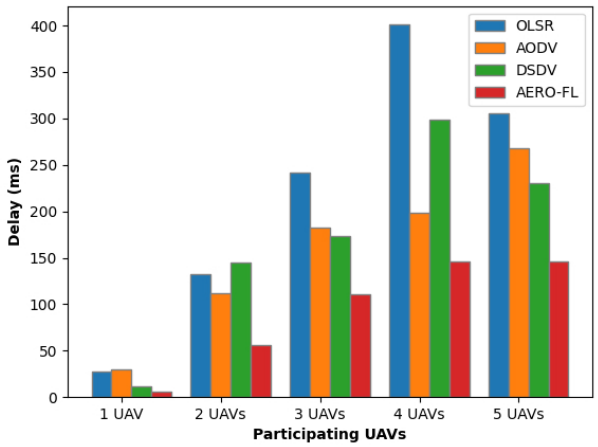


**FIGURE 14.** Performance of the application layer in terms of delay.

ratio close to 95%, followed by OLSR with a packet delivery ratio exceeding 84%. In comparison, AODV and DSDV exhibit slightly lower performance, with DSDV recording the lowest packet delivery ratio at approximately 71%. As the number of UAVs in the network increases, the disparity between AERO-FL and the other protocols becomes more pronounced. OLSR, AODV, and DSDV experience a significant drop in performance, with packet delivery ratio for both AODV and DSDV falling below 70% when two UAVs are present. AERO-FL, however, maintains consistently high delivery rates, indicating its ability to scale effectively as additional UAVs join the network. Under the most challenging scenario involving five UAVs, OLSR, AODV, and DSDV suffer further reductions in performance, with packet delivery ratio values dropping below 50%. In contrast, AERO-FL continues to exhibit robust performance, sustaining a packet delivery ratio of nearly 80%.

### B. CUMULATIVE DELAY

The bar chart in Fig. (14) illustrates the application layer's performance concerning cumulative delay, taking into account the routing protocols under examination and the varying number of UAVs involved in the mission.

The findings demonstrate that AERO-FL consistently outperforms other routing protocols in terms of cumulative delay. With a single UAV in the network, all protocols achieve minimal delay, with AERO-FL achieving the smallest delay value. As the network expands to two UAVs, delay increases across all protocols, but AERO-FL maintains a significantly lower delay compared to OLSR, AODV, and DSDV. While the delays for the latter protocols range between 112 ms and 145 ms, AERO-FL remains around 56 ms. As the number of participating UAVs increases to three, four, and five UAVs, the delays for the other protocols, particularly OLSR, escalate sharply, exceeding 400 ms for 4 UAVs. In contrast, AERO-FL demonstrates superior scalability, keeping delay values below 145 ms even in the most challenging scenario with five UAVs.

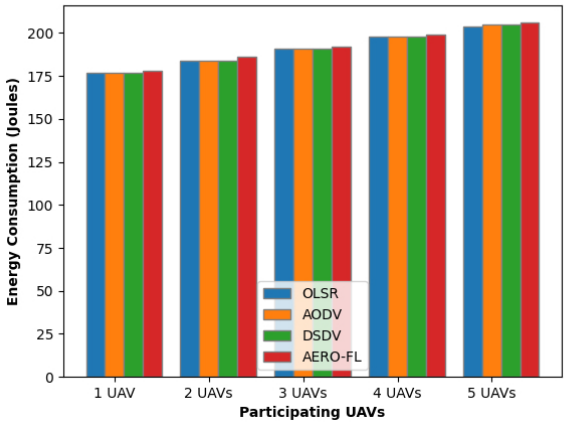


**FIGURE 15.** Performance of the application layer in terms of average energy consumption per node.

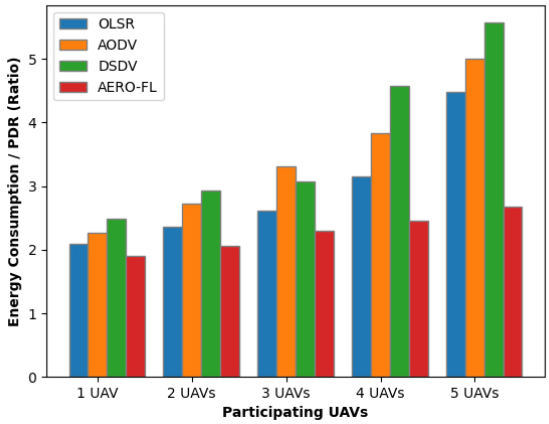


**FIGURE 16.** Performance of the application layer in terms of normalized average energy consumption per node.

### C. ENERGY CONSUMPTION AND ENERGY EFFICIENCY

This study also examines the average energy consumption per ad hoc node, as shown in Fig. (15), and in Fig. (16). Two different metrics are utilized to evaluate the energy efficiency and consumption per protocol. The objective is to investigate the interplay between adjustable transmission power and messaging intervals and their impact on the energy usage of individual nodes. As the number of UAVs increases, the average energy consumption per node also rises. Fig. (15) highlights this relationship, demonstrating a direct correlation between the addition of UAVs and increased energy consumption. For a single UAV, energy usage is relatively uniform across all protocols, indicating comparable baseline energy efficiency under minimal network load. However, as the network grows, energy consumption exhibits a gradual increase due to the heightened energy demands of additional UAVs.

The adaptive transmission power employed by the AERO-FL protocol results in slightly higher energy consumption than fixed-power approaches. Nevertheless, this strategy significantly enhances the packet delivery ratio across all scenarios, as depicted in Fig. (16). Specifically, with a single UAV, AERO-FL achieves the best performance

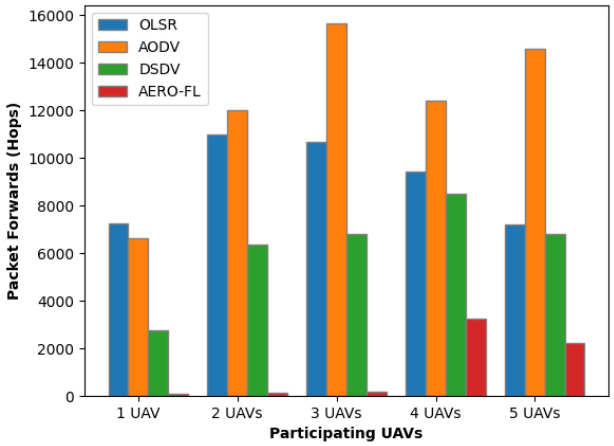


**FIGURE 17.** Performance of the application layer in terms of packet forwarding.

by maintaining a lower NEC ratio than competing protocols. This indicates the ability of AERO-FL to efficiently manage transmission power while optimizing energy efficiency. For two UAVs, AERO-FL continues to exhibit the lowest NEC ratio, outperforming OLSR, AODV, and DSDV, which demonstrate higher values. This trend becomes more pronounced as the number of UAVs increases to three and four. When five UAVs are involved, AERO-FL remains the most energy-efficient, while the other protocols experience a substantial rise in the respective values. These results demonstrate that although dynamic transmission power consumes slightly more energy than fixed transmission power, the energy is utilized far more effectively and significantly enhances network performance.

The rationale behind measuring average energy consumption per node, rather than system-wide, is to isolate the impact of transmission power on energy consumption, excluding other energy-consuming factors within the network. For instance, packet forwarding can significantly increase the system's overall energy consumption, for example, fewer hops mean fewer nodes are active, leading to reduced energy consumption system-wide.

### D. NUMBER OF PACKET FORWARDS

The line chart depicted in Fig. (17) showcases the magnitude of packet forwarding directed towards the destination across varying routing protocols and different quantities of UAVs.

In terms of packet forwarding measured by hops, AERO-FL demonstrates superior performance, achieving 96% fewer hops with one UAV, 97% fewer with two UAVs, 97% fewer with three UAVs, 62% fewer with four UAVs, and 67% fewer with five UAVs compared with the second best option in each scenario.

## IX. CONCLUSION

The majority of recent studies in FANET routing protocols have primarily focused on stochastic UAV movement. However, recent literature highlights that random movement models, such as Random Walk or Gauss Markov, do not accurately represent UAV behavior, as UAVs are typically airborne with specific objectives. This shift in understanding underscores the need for new routing protocols capable of supporting FANETs in real-world applications. The concept of mission-oriented routing protocols aptly describes this emerging requirement.

In this paper, we examined an agricultural management scenario, as it currently exists, involving a single UAV surveying an extensive crop area. This UAV lacks real-time data transmission capabilities and faces operational challenges such as battery recharges and potential failures, jeopardizing the mission on multiple fronts.

The findings of our work suggest that it is quite possible to use an FANET with the new proposed AERO-FL protocol, instead of a single-UAV system, which can significantly speed up the required time. Thus, our goal is to replace the single UAV system with an FANET that can complete the mission in a fraction of the time, potentially half, a third, a quarter, or even a fifth of the time required by a single UAV. Additionally, the FANET system will support real-time data transmission through a network of static ground nodes, enabling the mission to be completed on site rather than through a post-field process, as traditionally done. To achieve this, a reactive routing protocol is developed that supports air-to-ground communication, leveraging fuzzy logic to make more intelligent routing decisions that optimize overall network performance. The proposed routing protocol outperforms well-established ad hoc routing protocols on various metrics, including packet delivery ratio, delay, efficient energy consumption, and number of forwards.

With the introduction of this mission-oriented routing protocol, specifically designed for scanning operations, a task commonly used in various fields such as traffic surveillance, environmental monitoring, disaster response, military reconnaissance, and search-and-rescue missions, we aim to set the stage for future mission-oriented routing protocols. These protocols have the potential to unlock all the capabilities of FANETs, enabling the completion of tasks more efficiently and effectively, thereby significantly contributing to societal prosperity.

## REFERENCES

[1] M. Hassanalian and A. Abdelkefi, "Classifications, applications, and design challenges of drones: A review," *Prog. Aerosp. Sci.*, vol. 91, pp. 99–131, May 2017.

[2] G. Kakamoukas, P. Sarigiannidis, and I. Moscholios, "High level drone application enabler: An open source architecture," in *Proc. 12th Int. Symp. Commun. Syst., Netw. Digit. Signal Process. (CSNDSP)*, Jul. 2020, pp. 1–4.

[3] S. A. H. Mohsan, M. A. Khan, F. Noor, I. Ullah, and M. H. Alsharif, "Towards the unmanned aerial vehicles (UAVs): A comprehensive review," *Drones*, vol. 6, no. 6, p. 147, Jun. 2022.

[4] S. H. Alsamhi, F. Afghah, R. Sahal, A. Hawbani, M. A. Al-Qaness, B. Lee, and M. Guizani, "Green Internet of Things using UAVs in B5G networks: A review of applications and strategies," *Ad Hoc Netw.*, vol. 117, Jun. 2021, Art. no. 102505.

[5] V. Hassija, V. Saxena, and V. Chamola, "Scheduling drone charging for multi-drone network based on consensus time-stamp and game theory," *Comput. Commun.*, vol. 149, pp. 51–61, Jan. 2020.

[6] P. C. Karavetsios and A. A. Economides, "Performance comparison of distributed routing algorithms in ad hoc mobile networks," *WSEAS Trans. Commun.*, vol. 3, no. 1, pp. 317–321, Jan. 2004.
[7] I. Bekmezci, O. K. Sahingoz, and Ş. Temel, "Flying ad-hoc networks (FANETs): A survey," *Ad Hoc Netw.*, vol. 11, no. 3, pp. 1254–1270, May 2013.
[8] O. K. Sahingoz, "Networking models in flying ad-hoc networks (FANETs): Concepts and challenges," *J. Intell. Robotic Syst.*, vol. 74, nos. 1–2, pp. 513–527, Apr. 2014.
[9] G. Kakamoukas, P. Sarigiannidis, A. Maropoulos, T. Lagkas, K. Zaralis, and C. Karaiskou, "Towards climate smart farming—A reference architecture for integrated farming systems," *Telecom*, vol. 2, no. 1, pp. 52–74, Feb. 2021.
[10] D. Pamucar, I. Gokasar, A. E. Torkayesh, M. Deveci, L. Martínez, and Q. Wu, "Prioritization of unmanned aerial vehicles in transportation systems using the integrated stratified fuzzy rough decision-making approach with the Hamacher operator," *Inf. Sci.*, vol. 622, pp. 374–404, Apr. 2023.
[11] J. Agrawal, M. Kapoor, and R. Tomar, "A novel unmanned aerial vehicle-sink enabled mobility model for military operations in sparse flying ad-hoc network," *Trans. Emerg. Telecommun. Technol.*, vol. 33, no. 5, p. 4466, May 2022.
[12] F. A. Almalki, S. B. Othman, H. Sakli, and M. Angelides, "Revolutionizing healthcare by coupling unmanned aerial vehicles (UAVs) to Internet of Medical Things (IoMT)," in *Digital Health Transformation With Blockchain and Artificial Intelligence*. Boca Raton, FL, USA: CRC Press, 2022, pp. 47–59.
[13] A. Bujari, C. E. Palazzi, and D. Ronzani, "FANET application scenarios and mobility models," in *Proc. 3rd Workshop Micro Aerial Vehicle Netw., Syst., Appl.*, Jun. 2017, pp. 43–46.
[14] O. S. Oubbati, A. Lakas, F. Zhou, M. Güneş, and M. B. Yagoubi, "A survey on position-based routing protocols for flying ad hoc networks (FANETs)," *Veh. Commun.*, vol. 10, pp. 29–56, Oct. 2017.
[15] M. Kaur, S. Verma, and Kavita, "Flying ad-hoc network (FANET): Challenges and routing protocols," *J. Comput. Theor. Nanoscience*, vol. 17, no. 6, pp. 2575–2581, Jun. 2020.
[16] T. Kim, S. Lee, K. H. Kim, and Y.-I. Jo, "FANET routing protocol analysis for multi-UAV-based reconnaissance mobility models," *Drones*, vol. 7, no. 3, p. 161, Feb. 2023.
[17] S. Bharany, S. Sharma, S. Badotra, O. I. Khalaf, Y. Alotaibi, S. Alghamdi, and F. Alassery, "Energy-efficient clustering scheme for flying ad-hoc networks using an optimized LEACH protocol," *Energies*, vol. 14, no. 19, p. 6016, Sep. 2021.
[18] A. Nayyar, "Flying adhoc network (FANETs): Simulation based performance comparison of routing protocols: AODV, DSDV, DSR, OLSR, AOMDV and HWMP," in *Proc. Int. Conf. Adv. Big Data, Comput. Data Commun. Syst. (icABCD)*, Aug. 2018, pp. 1–9.
[19] G. A. Kakamoukas, P. G. Sarigiannidis, and A. A. Economides, "FANETs in agriculture—A routing protocol survey," *Internet Things*, vol. 18, May 2022, Art. no. 100183.
[20] I. D. Chakeres and E. M. Belding-Royer, "AODV routing protocol implementation design," in *Proc. 24th Int. Conf. Distrib. Comput. Syst. Workshops*, 2004, pp. 698–703.
[21] S. Choudhary, V. Narayan, M. Faiz, and S. Pramanik, "Fuzzy approach-based stable energy-efficient AODV routing protocol in mobile ad hoc networks," in *Software Defined Networking for Ad Hoc Networks*. Cham, Switzerland: Springer, 2022, pp. 125–139.
[22] J. Li, M. Wang, P. Zhu, D. Wang, and X. You, "Highly reliable fuzzy-logic-assisted AODV routing algorithm for mobile ad hoc networks," *Sensors*, vol. 21, no. 17, p. 5965, Sep. 2021.
[23] I. Alameri, J. Komarkova, T. Al-Hadhrami, and H. Alkaraawi, "Fuzzy logic-based congestion control in AODV mesh networks," in *Proc. 3rd Int. Conf. Electr., Comput., Commun. Mechatronics Eng. (ICECCME)*, Jul. 2023, pp. 1–10.
[24] R. Mehta, "Multivariate fuzzy logic-based ad hoc on-demand distance vector protocol under the impact of node mobility in wireless ad hoc networks," *Int. J. Commun. Syst.*, vol. 35, no. 14, p. e5264, Sep. 2022.
[25] S. T. Miri and S. Tabatabaei, "Improved routing vehicular ad-hoc networks (VANETs) based on mobility and bandwidth available criteria using fuzzy logic," *Wireless Pers. Commun.*, vol. 113, no. 2, pp. 1263–1278, Jul. 2020.
[26] R. Subha and H. Anandakumar, "Adaptive fuzzy logic inspired path longevity factor-based forecasting model reliable routing in MANETs," *Sensors Int.*, vol. 3, Jan. 2022, Art. no. 100201.
[27] F. Safari, H. Kunze, J. Ernst, and D. Gillis, "A novel cross-layer adaptive fuzzy-based ad hoc on-demand distance vector routing protocol for MANETs," *IEEE Access*, vol. 11, pp. 50805–50822, 2023.
[28] A. M. Rahmani, S. Ali, E. Yousefpoor, M. S. Yousefpoor, D. Javaheri, P. Lalbakhsh, O. H. Ahmed, M. Hosseinzadeh, and S.-W. Lee, "OLSR+: A new routing method based on fuzzy logic in flying ad-hoc networks (FANETs)," *Veh. Commun.*, vol. 36, Aug. 2022, Art. no. 100489.
[29] S.-W. Lee, S. Ali, M. S. Yousefpoor, E. Yousefpoor, P. Lalbakhsh, D. Javaheri, A. M. Rahmani, and M. Hosseinzadeh, "An energy-aware and predictive fuzzy logic-based routing scheme in flying ad hoc networks (FANETs)," *IEEE Access*, vol. 9, pp. 129977–130005, 2021.
[30] Q. Yang, S.-J. Jang, and S.-J. Yoo, "Q-learning-based fuzzy logic for multi-objective routing algorithm in flying ad hoc networks," *Wireless Pers. Commun.*, vol. 113, no. 1, pp. 115–138, Jul. 2020.
[31] S. Khan, M. Z. Khan, P. Khan, G. Mehmood, A. Khan, and M. Fayaz, "An Ant-Hocnet routing protocol based on optimized fuzzy logic for swarm of UAVs in FANET," *Wireless Commun. Mobile Comput.*, vol. 2022, pp. 1–12, Jun. 2022.
[32] P. Rajankumar, P. Nimisha, and P. Kamboj, "A comparative study and simulation of AODV MANET routing protocol in NS2 & NS3," in *Proc. Int. Conf. Comput. Sustain. Global Develop. (INDIACom)*, Mar. 2014, pp. 889–894.
[33] A. R. Rajeswari, "A mobile ad hoc network routing protocols: A comparative study," *Recent trends Commun. Netw.*, vol. 6, no. 1, pp. 1–24, Jul. 2020.
[34] R. A. Nazib and S. Moh, "Routing protocols for unmanned aerial vehicle-aided vehicular ad hoc networks: A survey," *IEEE Access*, vol. 8, pp. 77535–77560, 2020.
[35] G. He, "Destination-sequenced distance vector (DSDV) protocol," Netw. Lab., Helsinki Univ. Technol., Espoo, Finland, Tech. Rep., 2002, vol. 135, pp. 1–9.
[36] T. Clausen and P. Jacquet, *RFC3626: Optimized Link State Routing Protocol (OLSR)*, document RFC3626, 2003.
[37] A. Choksi and M. Shah, "Power constrained performance evaluation of AODV, OLSR and DSDV routing protocols for vehicular ad-hoc networks," in *Proc. Int. e-Conf. Intell. Syst. Signal Process. (e-ISSP)*. Cham, Switzerland: Springer, Aug. 2021, pp. 713–725.
[38] X. Chen, J. Tang, and S. Lao, "Review of unmanned aerial vehicle swarm communication architectures and routing protocols," *Appl. Sci.*, vol. 10, no. 10, p. 3661, May 2020.
[39] A. Rovira-Sugranes, A. Razi, F. Afghah, and J. Chakareski, "A review of AI-enabled routing protocols for UAV networks: Trends, challenges, and future outlook," *Ad Hoc Netw.*, vol. 130, May 2022, Art. no. 102790.
[40] L. A. Zadeh, "Fuzzy logic," in *Granular, Fuzzy, and Soft Computing*. Cham, Switzerland: Springer, 2023, pp. 19–49.
[41] P. Radoglou-Grammatikis, P. Sarigiannidis, T. Lagkas, and I. Moscholios, "A compilation of UAV applications for precision agriculture," *Comput. Netw.*, vol. 172, May 2020, Art. no. 107148.
[42] G. Livanos, D. Ramnalis, V. Polychronos, P. Balomenou, P. Sarigiannidis, G. Kakamoukas, T. Karamitsou, P. Angelidis, and M. Zervakis, "Extraction of reflectance maps for smart farming applications using unmanned aerial vehicles," in *Proc. 12th Int. Symp. Commun. Syst., Netw. Digit. Signal Process. (CSNDSP)*, Jul. 2020, pp. 1–6.
[43] S. Gangopadhyay and V. K. Jain, "A position-based modified OLSR routing protocol for flying ad hoc networks," *IEEE Trans. Veh. Technol.*, vol. 72, no. 9, pp. 12087–12098, Sep. 2023.
[44] U. Paul, R. Crepaldi, J. Lee, S.-J. Lee, and R. Etkin, "Characterizing WiFi link performance in open outdoor networks," in *Proc. 8th Annu. IEEE Commun. Soc. Conf. Sensor, Mesh Ad Hoc Commun. Netw.*, Jun. 2011, pp. 251–259.
[45] C. Samara, E. Karapistoli, and A. A. Economides, "Performance comparison of MANET routing protocols based on real-life scenarios," in *Proc. 4th Int. Congr. Ultra Modern Telecommun. Control Syst.*, Oct. 2012, pp. 870–877.
[46] X. Li and J. Yan, "LEPR: Link stability estimation-based preemptive routing protocol for flying ad hoc networks," in *Proc. IEEE Symp. Comput. Commun. (ISCC)*, Jul. 2017, pp. 1079–1084.
[47] nsnam. *The Network Simulator 3*. Accessed: Nov. 1, 2025. [Online]. Available: https://www.nsnam.org/
[48] usnistgov. *usnistgov/NetSimulyzer: A Flexible 3D Visualizer for Displaying, Debugging, Presenting, and Understanding NS-3 Scenarios*. Accessed: Nov. 1, 2025. [Online]. Available: https://github.com/usnistgov/NetSimulyzer

**GEORGIOS A. KAKAMOUKAS** received the Diploma degree in computer and telecommunications engineering from the Department of Informatics and Telecommunications, University of Western Macedonia, Greece, in 2013, and the M.Sc. degree in information and communication technology from International Hellenic University, in 2015. He is currently pursuing the Ph.D. degree in flying ad-hoc networks (FANETs) with the University of Western Macedonia. His main research interests include FANET communication protocols, FANET deployment in smart agriculture applications, supervised and unsupervised machine learning and big data analytics, and edge-fog computing.

**THOMAS D. LAGKAS** is currently an Assistant Professor with the Department of Computer Science, International Hellenic University, and the Director of the Laboratory of Industrial and Educational Embedded Systems. He was a Lecturer and then a Senior Lecturer with the Computer Science Department, International Faculty, The University of Sheffield, from 2012 to 2019. He was the Departmental Research Director and the Leader of the ICT Track of the South-East European Research Centre. Furthermore, he was an Adjunct Lecturer with the Department of Informatics and Telecommunications Engineering, University of Western Macedonia, from 2007 to 2013. Moreover, he was a Laboratory Associate and then a Scientific Associate with the Technological Educational Institute of Thessaloniki, from 2004 to 2012.

**VASILEIOS ARGYRIOU** received the B.Sc. degree in computer science from the Aristotle University of Thessaloniki, Greece, and the M.Sc. and Ph.D. degrees in electrical engineering working on registration from the University of Surrey. He joined the Communications and Signal Processing (CSP) Department, Imperial College London, London, where he was a Research Fellow working on 3-D object reconstruction. He is currently a Professor with Kingston University working on computer vision and AI for crowd and human behavior recognition, anomaly detection, scene analysis, and serious computer games for medical applications. Also his research is conducted on AI-powered augmented and virtual reality (AR/VR) systems.

**SOTIRIOS K. GOUDOS** (Senior Member, IEEE) is currently a Professor with the Department of Physics, Aristotle University of Thessaloniki, Greece. His research interests include antenna and microwave structure design, evolutionary algorithms, wireless communications, and semantic web technologies. He is also the Director of the ELEDIA@AUTH Laboratory Member of the ELEDIA Research Center Network. He is also the Founding Editor-in-Chief of the *Telecom* open access journal (MDPI publishing). He is currently serving as the IEEE Greece Section Vice-Chair. He is the author of the book *Emerging Evolutionary Algorithms for Antennas and Wireless Communications*, Institution of Engineering & Technology, in 2021. He is currently serving as an Associate Editor for IEEE TRANSACTIONS ON ANTENNAS AND PROPAGATION, IEEE ACCESS, and IEEE OPEN JOURNAL OF THE COMMUNICATION SOCIETY.

**PANAGIOTIS RADOGLOU-GRAMMATIKIS** (Member, IEEE) received the Diploma (M.Eng.) and Ph.D. degrees from the Department of Informatics and Telecommunications Engineering (now Department of Electrical and Computer Engineering), Faculty of Engineering, University of Western Macedonia, Greece, in 2016 and 2023, respectively. His main research interests include cybersecurity and mainly focus on cyber-AI, intrusion detection, and security games. He has published more than 40 research papers in international scientific journals, conferences, and book chapters, including IEEE TRANSACTIONS ON INDUSTRIAL INFORMATICS, IEEE TRANSACTIONS ON NETWORK AND SERVICE MANAGEMENT, IEEE TRANSACTIONS ON EMERGING TOPICS IN COMPUTING, and *Computer Networks* (Elsevier). He was included in Stanford University's List (shared by Elsevier) of the Top 2% of Scientists in the World for 2021 and 2022. He is also a Postdoctoral Researcher with the ITHACA Laboratory, University of Western Macedonia, participating in several national and European-funded research projects, such as H2020 SPEAR, H2020 SDN-microSENSE, H2020 TERMINET, H2020 EVIDENT, H2020 ELECTRON, AI4CYBER, and DYNABIC.

**STAMATIA BIBI** received the B.Sc. degree in informatics and the Ph.D. degree in software engineering from the Aristotle University of Thessaloniki, Greece, in 2002 and 2008, respectively. She is currently an Associate Professor in software engineering with the Department of Electrical and Computer Engineering, University of Western Macedonia, Kozani, Greece. She serves/served as a program committee member for various international conferences and as a Referee for journals in the fields of software engineering, such as *Journal of Systems and Software*, *Information and Software Technology*, IEEE TRANSACTIONS ON SOFTWARE ENGINEERING, and IEEE SOFTWARE. She has published more than 60 articles in international journals and conferences. She is/was involved in more than 20 research and development ICT projects, with funding from national and international organizations. Her research interests include software process models, cost estimation, quality assessment, and data analysis methods for software engineering.

**PANAGIOTIS G. SARIGIANNIDIS** (Member, IEEE) received the B.Sc. and Ph.D. degrees in computer science from the Aristotle University of Thessaloniki, Thessaloniki, Greece, in 2001 and 2007, respectively. He is currently the Director of the ITHACA Laboratory, the Co-Founder of the first spin-off of the University of Western Macedonia, Kozani, Greece: MetaMind Innovations P.C., and an Associate Professor with the Department of Electrical and Computer Engineering, University of Western Macedonia. He has published over 220 papers in international journals, conferences, and book chapters. His research interests include telecommunication networks, the Internet of Things, and network security. He participates in the editorial boards of various journals, including *International Journal of Communication Systems* and *EURASIP Journal on Wireless Communications and Networking*.